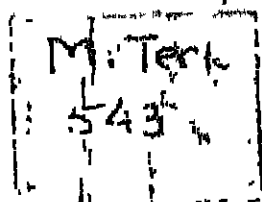


NONLINEAR FLOW THROUGH POROUS MEDIA

BY

P. JAGADEESHA RAO

S43 TH
CE/1971/M
R18n



DEPARTMENT OF CIVIL ENGINEERING

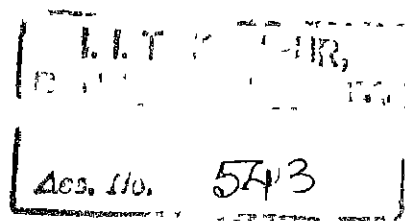
INDIAN INSTITUTE OF TECHNOLOGY KANPUR

♦ JULY 1971

CE
1971
M
RAO
Non

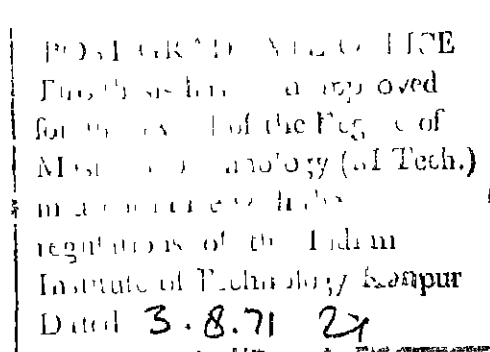
NONLINEAR FLOW THROUGH POROUS MEDIA

A Thesis Submitted
In Partial Fulfilment of the Requirements
for the Degree of
MASTER OF TECHNOLOGY



CE-1771-17-P.D.N

BY
P JAGADEESHA RAO



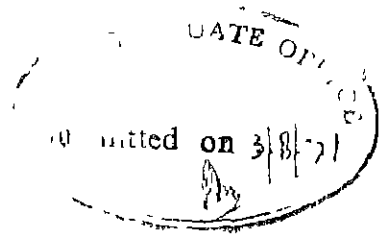
to the

DEPARTMENT OF CIVIL ENGINEERING
INDIAN INSTITUTE OF TECHNOLOGY KANPUR
JULY 1971

7.8.71
S. S. S. S.
12/8/71



CERTIFICATE



Certified that this work, "Nonlinear Flow Through Porous Media" by P. Jagadeesha Rao, has been carried out under my supervision and that this work has not been submitted elsewhere for a degree.

K. Subramanya

DR. K. SUBRAMANYA
Assistant Professor
Department of Civil Engineering
Indian Institute of Technology,
Kanpur

RECEIVED
The undersigned is pleased
to certify that the work
done by P. Jagadeesha Rao, on
Nonlinear Flow Through Porous Media,
in accordance with the
regulations of the Indian
Institute of Technology Kanpur
Dated 3 8 71 24

ACKNOWLEDGEMENTS

The author wishes to gratefully acknowledge the encouragement and invaluable help of Dr. K.Subramanya under whose guidance this thesis work was carried out.

The author is also thankful to Dr. A.J.Valdsangkar for his suggestions and discussions. The author expresses his appreciation to the staff of Hydraulic Engineering Laboratory, Department of Civil Engineering for their cooperation.

P. Jagadeesha Rao

TABLE OF CONTENTS

	Page
List of Figures	
Notations Used	
Abstract	
Chapter I Introduction and Literature Review	1
1.1 Introduction	1
1.2 Literature Review	2
1.2.1 Nonlinear Equations	2
1.2.2 The Beginning of Nonlinear Flow	5
1.2.3 Friction Factor in Porous Media Flow	9
1.2.4 Nonlinear Coefficients	12
1.2.5 Analytical and Experimental Investigations	13
Chapter II Analytical Solutions to Some Non-Darcy	
Flow Problems	16
2.1.1 Flow Into a Trench - Artesian Flow Case(1)	16
2.1.2 Profile of the Phreatic Surface	18
2.1.3 Case (11) : Solution by Using Power Law	20
2.2.1 Flow Into a Trench - Gravity Flow	21
2.2.2 Variation of Discharge with Drawdown	
Ratio	23
2.2.3 Case (11) : Solution by Power Law	24

2.3.1	Flow Into a Trench - Combined Artesian and Gravity Flow	25
2.4.1	Radial Flow Into a Well Completely Penetrating a Confined aquifer Case (1)	29
2.4.2	Case (11) Power Law Solution	31
2.5.1	Radial Flow Into a Well Completely Penetrating an Unconfined Aquifer (Gravity Flow) Case (1)	32
2.5.2	Case (11) Power Law Solution	35
Chapter III Study of Non-linear Flow		53
3.1	Purpose of the Experiment	53
3.2	Experimental Set-up	53
3.3	Procedure	54
3.4	Results and Discussion	56
Chapter IV Nonlinear Flow Through Non-homogenous Porous Media		69
4.1	Introduction	69
4.2	Analysis	70
4.3	Experimental Verification Flow Normal to Stratification	73
4.4	Results and Discussion	73
4.5	Head Loss Through Gravel Packs for Tube Wells	74

4.6 Analysis for Flow Through Two Layers of Pockin_	74
Chapter V Conclusions	78
List of References	80
Appendix - A Tables	1
Appendix - B Head Loss Through Gravel	
Back-Illustration	xx
Appendix - C Wall Effects in Permeameters	xxi

LIST OF FIGURES

<u>Figure Number</u>	<u>Description</u>	<u>Page</u>
1.	Definition Sketch Confined Trench Flow	37
2.	Definition Sketch - Unconfined Trench Flow	37
3.	Definition Sketch - Confined - Unconfined Trench Flow	37
4.	Confined Trench Flow (Forchheimers Equation)	38
5.	Confined Trench Flow (Forchheimers Equation)	39
6.	Confined Trench Flow (Power Law)	40
7.	Unconfined Trench Flow (Forchheimers Equation)	41
8.	Unconfined Trench Flow (Forchheimers Equation)	42
9.	Unconfined Trench Flow (Power Law)	43
10.	Combined Artesian - Gravity Trench Flow (Power Law)	44
11.	Definition Sketch - Artesian Well Flow	45
12.	Definition Sketch - Gravity Well Flow	45
13.	Artesian Well Flow (Forchheimers Equation)	46
14.	Artesian Well Flow (Power Law)	47
15.	Unconfined Well Flow (Forchheimers Equation)	48
16.	Unconfined Well Flow (Forchheimers Equation)	49
17.	Unconfined Well Flow (Forchheimers Equation)	50
18.	Unconfined Well Flow (Forchheimers Equation)	51
19.	Unconfined Well Flow (Power Law)	52

20.	Schematic Diagram of the Experimental Setup	60
21.	Details of Permeameter	60
22.	Grain Size Distribution of River Gravel	61
23.	Variation of $1/V$ with V .	62
24.	Variation of Friction Factor with Reynolds number	63
25.	Variation of Coefficient 'a' with Specific Permeability	64
26.	Variation of Coefficient 'a' with Specific Permeability	65
27.	Variation of Coefficient 'b' with Specific Permeability	66
28.	Variation of Coefficient 'b' with Specific Permeability	67
29.	Relation of Specific Permeability to Particle Size for nearly Uniform Porous Media	68
30.	Definition Sketch - Nonhomogeneous Porous Media	68

NOTATIONS USED

A = Area

A_1 = Area of Inner Zone

A_w = Area of Wall Zone

a, b = Nonlinear Coefficients

a_w, b_w = Nonlinear Coefficients for Wall Zone

$a_1, b_1, a_2, b_2 \dots$ = Nonlinear Coefficients for Different
Layers

a_x, b_x = Equivalent Nonlinear Coefficients in the X
Direction

a_y, b_y = Equivalent Nonlinear Coefficient in the Y
Direction

C = Coefficient in the Equation (1.3)

C_1, C_2, C_3 = Coefficients Depending on the Physical
Properties of the Media

d_1, d_2 = Thickness of the Layers

d' = Total Thickness of the Layers

d_{50} = Median Particle Size

D = Depth

D_1 = Diameter of the Permeameter Tube

e = Void Ratio

F, F_1, F_2, F_3 = Friction Factors

F = $2g d_{50} i/v^2$

F_1 = $g C_2 d i/v^2$

F_2 = $g d i/v^2$

F_3 = $(1/R_e) + 0.55 C_3^{1/2}$

g = Acceleration of Gravity

h = Piezometric Head at Any Point

h_e = Head at the Face of the Trench or Well

H = Piezometric Head at Distance L or R

H_T = Total Head

H_1 = h/h_e

i = Hydraulic Gradient

k = Specific Permeability

K = Darcys Coefficient of Permeability

l = Characteristic Length of Flow

L = Distance

L_Q = Distance at which Flow Changes from
Gravity to Artesian Type

m = Exponent in the Equation (1.3)

m_1, m_2 = Fractions

n = Porosity

$$n_1 = 1/m$$

$$N = \text{Number of Layers}$$

$$\Delta P = \text{Pressure Drop}$$

$$q_L = \text{Linear Discharge/Unit Width}$$

$$q = \text{Nonlinear Discharge/Unit Width}$$

$$Q_-, Q_{+1}, Q_{+2} = \text{Nonlinear Discharge (Dimensionless)}$$

$$Q_- = qa/\pi h_e^2$$

$$Q_{+1} = qa/D$$

$$Q_{+2} = aq/h_e$$

$$Q_d, Q_{d+1} = \text{Linear Discharge (Dimensionless)}$$

$$Q_d = Q_L / (h_e^2 \pi K)$$

$$Q_{d+1} = q_L/KD$$

$$r_w = \text{Radius of Well}$$

$$r = \text{Any Distance From the Center of the Well } (0 < r < R)$$

$$r_{d1} = h_e/H$$

$$r_{d2} = h_e/D$$

$$r_{d3} = H/r_w$$

$$r_{d4} = r_w/h_e$$

$$r_h = \text{Hydraulic Mean Radius}$$

R_e, R_1 = Reynolds Numbers

$$R_e = v_d d_{50} / \nu$$

$$R_1 = V_V d_{50} / \nu$$

$$R_1 = r / c_{\infty}$$

S = Distance Measured in the Direction of Velocity

t_1, t_2 = Thickness of Gravel Pack Layers

t = Thickness of Wall Zone

V = Average Velocity

V_V = Void Velocity

v_1 = Velocity in the Inner Zone

V_w = Velocity in the Wall Zone

y = Distance ($0 < y < L$)

Z = h/H

\mathcal{J}_r = Discharge ratio (Q/Q_L)

$\mathcal{A}_0, \mathcal{B}_0$ = Constants

$\eta_1, \eta_2, \eta_3, \eta_4, \eta_5, \eta_6, \eta_7, \eta_8$ = Nonlinearity Parameters

$$\eta_1 = (b/a^2) \left(\frac{H - h_e}{L} \right)$$

$$\eta_2 = b/a^2$$

$$\eta_3 = \frac{H - h_e}{L}$$

$$\eta_4 = \frac{CL}{h_e}$$

$$\eta_5 = \frac{H-L}{C(I-L_G)}$$

$$\eta_6 = (b/c^2) \left(\frac{H-h_e}{R} \right)$$

$$\eta_7 = CR/(H-h_e)$$

$$\eta_8 = \frac{r_w C}{h_e}$$

$$\gamma = \text{Specific Weight of the Fluid}$$

$$\rho = \text{Density of the Fluid}$$

$$\mu = \text{Dynamic Viscosity of the Fluid}$$

$$\nu = \text{Kinematic Viscosity of the Fluid}$$

ABSTRACT

Deviations from Darcy type ^{of flow} are observed in many field situations. As such it has become necessary to use head loss equations suggested by Forchheimer and Hirschbach for realistic analysis of such problems. A review of the literature on the subject of Non-linear Flow Through Porous Media is presented. Analytical solutions to some of the non-Darcy type of flow problems are presented based on Dupuits assumption. The effect of nonlinearity parameter on discharge ratio and draw-down curve are discussed in detail. Equations are developed for nonlinear flow through nonhomogenous porous Media. ✓

✓ The experimental investigations of nonlinear coefficients a and b for various materials are presented. A method of predicting the values of a and b using the available data is suggested. Equations developed for nonlinear flow through nonhomogenous porous media are verified experimentally for a two layer gravel bed. The estimation of head loss through gravel pack for a tube well is illustrated. ✓

CHAPTER I

INTRODUCTION

1.1 The problems involving flow of water through porous media are very widely in scope and its engineering applications. Traditionally these problems have been solved based on Darcy's linear relationship between head loss and velocity :

$$V = K_1 \quad (1.1)$$

where K_1 = Darcy's coefficient of permeability.

$$i = - \frac{dH_p}{ds} = \text{Negative hydraulic gradient}$$

H_p = Total head i.e. sum of the piezometric and velocity heads.

s = Distance measured in the direction of velocity

V = Bulk or average seepage velocity.

The equation (1.1) satisfactorily describes the flow conditions, provided velocities are small i.e. the flow is laminar. However, as the velocity of flow, particle size and Reynolds number increase Darcy's linear

relationship leads to inaccurate predictions. Thus while many practical problems of flow through porous materials can be solved accurately based on Darcy's law, various field situations have been observed where a more accurate relationship between head loss and velocity must be employed to obtain realistic solutions.

Some of the situations where in the use of nonlinear relationship becomes necessary are :

- (1) Flow in the area adjacent to a pumping well especially in a coarse grained aquifer.
- (2) Flow in the filter packs (gravel packs) of tube wells.
- (3) Flow through rock fill banks and dams.
- (4) Flow through filters used in water purification plants.

In the recent years, many investigators have studied ground water flow problems involving nonlinear flow situations. However, the analysis is far from complete, as such an attempt has been made in this investigation to analyse some of the nonlinear flow problems and to verify the equations developed for nonlinear flow through nonhomogeneous medium.

1.2 Literature Review

1.2.1 Non-linear Equations

The non-Darcy regime of flow has been generally described by the equation suggested by Forchheimer,

$$i = aV + bV^2 \quad (1.2)$$

in which a and b are constants determined by the properties of the fluid and porous media. Number of authors (Volker - 1968), (Ahmed & Sunada - 1969), (O'Neill, Parkin, Todd, Tyagi, Ranganadha Rao & Suresh - 1970) have supported this relationship after conducting experimental investigations. By deduction from Navier Stokes equation Ahmed and Sunada (1969) showed that the governing head loss equation is of the form suggested by Forchheimer, i.e. equation (1.2), but values of coefficients a and b are not strictly constant and depend on the Reynolds number of the flow. However, the available data indicates that a and b are essentially constants over a range of Reynolds numbers.

Another form of equation suggested by Missbach :

$$i = cV^m \quad (1.3)$$

is also in common use. In this equation, C is a coefficient determined by the properties of the fluid and medium.

m = An exponent lying between 1.0 and 2.0 The value of m varies from 1.0 for laminar flow to 2.0 for completely turbulent flow.

The use of equation (1.3) is supported by many authors. (Anandakrishnan, Varadarajulu - 1963), (Parkin, Trollope, Lawson - 1966).

Wilkins (1955), using wide range of aggregate sizes and marbles, derived the equation of the form.

$$V_V = C_1 \mu^{\alpha_1} r_*^{\beta_1} n_1 \quad (1.4)$$

where V_V = Seepage velocity

$$n_1 = \frac{1}{m}$$

r_* = Hydraulic mean radius

$$= \frac{\text{Void ratio}}{\text{Surface area per unit volume}}$$

μ = Dynamic viscosity of the fluid

C_1, α_1, β_1 — are constants.

The value of C_1 , varied from 32.9 for crushed stone to 46.5 for marbles in inch units.

1.2.2 The Beginning of Non-linear Flow

The accepted method of expressing the limitations to Darcy's law has been by pipe analogy to determine the Reynolds number at the point where departure from the linear relationship is first noted. It is well known that the Reynolds number

$$Re = \frac{\rho V l}{\mu} \quad (1.5)$$

where ρ = Density of the fluid
 μ = Dynamic viscosity of the fluid
 l = Characteristic length of flow i.e median size (d_{50}) of the particle.

While calculating Reynolds number (Re_1) some investigators (Parkin, Lawson, Trallo e - 1966) used seepage velocity which is function of porosity (n).

Seepage velocity or void velocity (V_v) is defined in terms of void ratio 'e'.

$$V_v = \frac{Q}{A} \frac{(1+e)}{e} \quad (1.6)$$

$$= \frac{\text{Total discharge}}{\text{Area of voids}}$$

where, A = Total area

Limiting values of Reynolds number (R_e) from 0.1 to 75.0 have been measured by various investigators (Anandakrishnan, Varadarajulu - 1963), (Wright - 1968), (Volker - 1969) (Ahmed, Gunada - 1969) for wide range of fluids and materials. The large variation in the Reynolds number (R_e) reflects in the deficiency of the usual form of parameter in accounting for the variables involved in the flow, such as particle size, shape, particle arrangement, roughness and porosity.

Eventhough the laminar flow through a porous media is considered analogous to the laminar flow through the pipe, the analogy does not hold good beyond linear regime of flow. The logarithmic plot of resistance coefficient (F) versus Reynolds number (R_e) does not show a sharp jump in the resistance coefficient found in the the case of pipes at the end of laminar regime. The plot, however exhibits a long progression from the stream line Darcy flow state in which head loss is proportional to the velocity, to a turbulent state in which the head loss varies as square of the velocity (Wright-1968),

(United, Sunada - 1969) The gradual transition found to exist between the regions of laminar and turbulent flow is probably due to the large variation in the particle size and voids within a given porous medium.

The limitations of pipe flow analogy is that in pipe flow the motion is along rectilinear paths at constant velocity for steady state condition. While in case of flow through porous media, the fluid undergoes continual cycles of acceleration and deceleration while following curvilinear paths.

The major difficulty in the definition of Reynolds number (R_e) is the length dimension. For pipe flow this dimension is clearly defined by pipe diameter, but for porous medium the flow channel is so variable in dimensions that a similar dimension is almost impossible. The effective particle size appears to be more significant than a flow path dimension.

Taylor (1948) calculated that for a unit hydraulic gradient, the maximum diameter of the uniform sand in which the laminar flow will occur is 0.5 m.m.

On the basis of the experimental results and interpretations of flow through porous media, Wright (1968) has classified the regimes of flow into four

categories as follows.

(1) A laminar regime in which at every point microvelocity is stationery and head loss is directly proportional to the velocity. The viscous forces predominate and maximum velocity occurs near the center of each flow passage.

(2) A steady ^cinter_λial regime in which at every point microvelocity is still stationery but head loss has ceased to vary linearly with velocity. Both viscous forces and interial actions influence the motion. Stationery vortices may be formed at the upper end of the regime.

(3) A turbulent transition regime in which the microvelocity fluctuates at any point with increasing but regular frequency and head loss approaches dependence on the square of the velocity.

(4) A fully turbulent regime in which all parts of the flow are turbulent, the microvelocity fluctuates randomly about a mean. The head loss is close to dependence on the square of the velocity but if a viscous sub-layer is present it will continue to decrease slightly as the flow increases.

Because of the Stochastic nature of flow through porous media, it is not to be expected that these regimes can be defined precisely. However following range of Reynolds number (R_e) can be generally accepted (Wright - 1968).

Regime	Reynolds number (R_e)
Laminar	1.0 - 5.0
Steady Inter ^t ial	90 - 120
Turbulent Transition	
Transition	about 800

Nonlinear equations can thus be considered to be valid for a region of Reynolds number (R_e) 10 - 2000 in which steady interial flow occurs.

1.2.3 Friction Factor in Porous Media Flow

Ahmed and Sunada (1969) showed that in porous media flow a unique relationship exists between two dimensionless parameters which are defined in terms of the physical properties of the fluid, porous medium and flow phenomena.

The equation derived by Ahmed and Sunada is of the form,

$$1 = \frac{1}{\rho g} \frac{dP}{dx} = - \frac{\mu}{\rho g k} v + \frac{1}{g \sqrt{C_2 k}} v^2 \quad (1.7)$$

$$\text{and } F_1 = \frac{1}{R_e} + 1.0 \quad (1.8)$$

where $\frac{dP}{dx}$ = Pressure gradient

$$\text{and } k = C_2 d^2 \quad (1.9)$$

k = Specific permeability

C_2 = Coefficient depending on the physical properties of the media.

d = Particle size

g = Acceleration due to gravity

$$\text{Friction factor } (F_1) = g C_2 d \frac{1}{v^2}$$

$$\text{The constants } a \text{ and } b \text{ are } \frac{\mu}{\rho g k} \text{ and } \frac{1}{g \sqrt{C_2 k}}$$

respectively.

The results of 18 tests by Ahmed and Sunada (1969) showed that a single relationship exists between friction factor (F_1) and Reynolds number (R_e). Nonlinearity becomes predominant at $R_e = 0.2$ and when R_e is large H approaches unity. However, they have not clearly mentioned the significance of the parameter C_2 , in the equation (1.7). If the range of the parameter C_2 are known from the experimental values for different materials, it would have been useful to determine the specific

permeability accurately and to check the relationship given by equation (1.8). Todd (1959) has defined friction factor as

$$F_2 = \frac{d \Delta P}{2 \rho L V^2} \quad (1.10)$$

$$= \frac{f d L}{2 V^2} \quad (1.11)$$

ΔP = Pressure drop over a length L . It has been shown that transition from laminar to turbulent flow occurs when R_e is in the range between 1 and 10, thus indicating an upper limit for the validity of Darcy's law.

Ward(1970) has defined friction factor as

$$F_3 = \frac{1}{R_e} + 0.55 C_3^{1/2} \quad (1.12)$$

The equation (1.12) is similar to the equation (1.8) except for the term $0.55 C_3^{1/2}$ where C_3 is variable depending on the physical properties of the media.

Ranganadha Rao and Suresh (1970) concluded from their experimental investigations that the relationship given by the equation (1.8) proves only the validity of Darcy's equation (1.3) but cannot prove the correctness of the values a and b calculated from hydraulic measurements.

Since friction factor (F) is variously defined by many investigators, Dudgeon (1964), Todd (1970), Ahmed and Sunada (1969), Ward (1970), there is a need for standardising a form of the friction factor. The friction factor (F_1) versus Reynolds number (Re) plot obtained by Ahmed and Sunada (1969) for different materials exhibits a single line relationship. Where as Dudgeon's plot shows different lines for various materials. The plot obtained by Todd and Tyagi (1970) also does not agree with Ahmed and Sunada's plot. For different porous materials at a particular Reynolds number (Re), friction factor (F) cannot be same since it is function of particle size, shape particle arrangement, roughness and porosity. Thus it appears the relationship between friction factor (F) and Reynolds number (Re) can be better represented by different lines for various materials.

1.2.4 Non-linear Coefficients - Values of a and b, c and m

Many investigators have obtained the values of a and b for different materials over wide range of Reynolds number. The values obtained by Dudgeon (1964), Sunada Ahmed (1969), Ranganadha Rao and Suresh (1970) are shown in tables (1), (2) and (3) respectively. Anandakrishnan and Varadarajulu (1963) obtained the values of $K' = \frac{1}{C}$ and m for different grades of sand (Table 4).

Volker (1969) obtained the values of a and b in Forchheimer's equation and C and m in exponential equation by laboratory studies of model gravel banks in an open flume.

While tabulating their values for coefficients a and b in the equation (1.2) and C and m in the equation (1.3), many investigators have not mentioned the range of Reynolds number over which the coefficients for various materials are valid. Since the coefficients are function of Reynolds number (R_e), porosity and other properties of the media and water, these results are of limited use in practical application. Proper shifting of the reported data and its classification is needed to make them useful in practical application. One of the aim of the present study is to present a method of predicting the value of a and b for a given porous media.

1.2.5 Analytical and Experimental Investigations

Many investigators (Parkin, Lawson, Trollope-1966)

(Robin Curtis - 1967), have studied the flow through rock fill banks and analysed the stability of slope against seepage. Parkin (1963) made extensive studies on model dams in a 4 feet wide flume and found the method of gradually varied flow is satisfactory to determine the water surface profiles. The flow of air

through porous media was studied by Wright (1968)%. Both velocity and turbulence measurements were made with the use of a hot wire anemometer. Wright's results show that although linear resistance relation cease to be valid at Reynolds number (R_e) of about 2.0, velocity fluctuations do not begin until Reynolds number (R_e) is about 100 and turbulence is not fully established until it is about 800. In another set, the flow of water through gravel bed in cylindrical and converging parameters was studied and results were compared. From the observations it is found that the resistance begins to deviate from Darcy's linear law when $R_e = 2.0$ and where $R_e = 100$, resistance increases to 3.5 times the laminar value. These observations confirm that Darcy's law cease to be valid before the onset of turbulence.

Volker (1969) carried out the experiments on flow of water through model gravel banks in an open flume. The experimental results were checked by finite element method. Dudgeon (1967) studied the wall effect in permeameter using cylindrical and box type permeameters. The errors due to wall effect ranging from 5 to 15% were measured for particle to permeameter tube diameter ratios from 1 : 5 to 1 : 250.

Rubins (1966,1969) made extensive study of nonlinear flow problems. He has presented an electrical analogue model for the solution of such problems.

Madhav and Subramanya (1970) have presented solutions to the some of the common seepage problems by using Forchheimer's and also Dupuit's assumption.

CHAPTER II

ANALYTICAL SOLUTIONS TO SOME NON-DARCY FLOW PROBLEMS

2.01 In this chapter solutions to some simple problems with non-Darcy flow situations are analysed by equations (1.2) and (1.3) and with the assumption, Dupit's theory to be valid.

2.1 Flow into a trench - Artesian Flow

Figure (1), shows a construction of a fully penetrating trench in a stratum under an artesian condition with all the relevant dimensions. In the development of this equation and subsequent equations, it has been assumed that Dupit - Foreheimer assumption (Leonards) holds good.

2.1.1 Case (1)

If Q is the discharge into the trench per unit time, then average velocity V is,

$$V = \frac{Q}{BD}$$

where B and D are width and depth of the previous stratum respectively.

Substituting the value of V in equation (1.2),

$$\begin{aligned} 1 &= \frac{dh}{dy} \\ &= \frac{aQ}{BD} + b \left(\frac{Q}{BD} \right)^2 \end{aligned} \quad (2.1)$$

where h is the height of water above the bottom of trench and y distance from the trench.

Integrating equation (2.1) for h with boundary conditions, at $y = 0$, $h = h_e$

$$h = h_e + \left\{ \frac{aQ}{BD} + b \left(\frac{Q}{BD} \right)^2 \right\} y \quad (2.2)$$

For boundary conditions at $y = L$, $h = H$ in the equation (2.2) and solving for Q

$$\left\{ \frac{b}{D^2 B^2} \right\} Q^2 + \frac{a}{DB} Q - \left(\frac{H - h_e}{L} \right) = 0 \quad (2.3)$$

where h_e and H are water level on the face of trench and at distance L from the trench respectively.

$$\text{With } Q = \alpha Q_L \text{ and } \eta_1 = \frac{b}{a^2} \left(\frac{H - h_e}{L} \right)$$

where Q_L is the flow into the trench for linear case i.e.

when $b = 0$, $Q_L = \frac{KDB}{L} (H - h_e)$ and η_1 is a parameter,

signifying the nonlinearity parameter b , the equation (2.3)

can be written into the following dimensionless form.

$$\eta_1 \alpha^2 + \alpha - 1 = 0 \quad (2.4)$$

in which $\alpha = Q/Q_L$ is the ratio of nonlinear discharge to linear discharge.

Solution of the equation (2.4) is shown in figure (4) for α as function of η_1 on semilog plot. For increasing values of η_1 i.e. increasing nonlinearity the actual discharge decreases logarithmically compared to the discharge estimated on the basis of linear law. Thus for any porous media defined by (a, b) increasing head $(H-h_e)$ do not proportionately increase discharge and value of discharge ratio decrease with increasing heads. Thus the effect of using Darcy law (linear law) for non-linear regime is to overestimate the expected discharge. The expression for drawdown curve obtained from equation (2.2) after substituting for Q is same as one obtained by using linear law i.e. $H-h = \frac{(H-h_e)(L-Y)}{L}$

2.1.2 Profile of the Phreatic Surface

The equation (2.2) can be written in the following form.

$$\frac{h}{h_e} = 1 + \left\{ \frac{aQ}{BD} + \frac{bQ^2}{B^2D^2} \right\} \frac{y}{h_e} \quad (2.5)$$

For unit width of trench, $B = 1$, the equation (2.5) can

be represented in the following form.

$$\frac{h}{h_e} = 1 + \left\{ Q_{d+1} + Q_{d+1}^2 \cdot \eta_2 \right\} \cdot \frac{y}{h_e} \quad (2.6)$$

where Q_{d+1} is equal to $\frac{q}{D}$, discharge (dimensionless) for nonlinear case and η_2 is the nonlinearity parameter i.e. b/a^2 .

q = Discharge per unit width of trench.

For linear case, the equation (2.6) reduces to

$$\frac{h}{h_e} = Q_{d+1} \cdot \frac{y}{h_e} + 1.0 \quad (2.7)$$

where Q_{d+1} is discharge (dimensionless) for linear case and equal to $\frac{q_L}{D}$.

q_L = Discharge per unit width of trench for linear case.

The solution of the equation (2.6) and (2.7) is represented in Figure (5) on semilogarithmic paper for $\frac{y}{h_e}$ versus $\frac{h}{h_e}$ with varying values of η_2 and same value of discharge (dimensionless). The effect of nonlinearity for same discharge is to increase the drawdown. For values of $\eta_2 > 0.010$, the increasing value of η_2 has significant effect on draw-down curve.

2.1.3 Case (11) : Solution by Using Power Law

In this case solution to the above mentioned problem is obtained by equation (1.3)

$$\begin{aligned} 1 &= \frac{dh}{dy} \\ &= cv^m \end{aligned}$$

Substituting the value of V in equation(13),

$$\frac{dh}{dy} = C \left(\frac{Q}{BD} \right)^m \quad (2.8)$$

Integrating equation (2.8) with boundary conditions $y = 0, h = h_e$ and $y = L, h = H$,

$$C \left(\frac{Q}{BD} \right)^m - \left(\frac{H-h_e}{L} \right) = 0 \quad (2.9)$$

with $\alpha = Q/Q_L$ and $\eta_3 = \frac{H-h_e}{LC}$

where $Q_L = KBD \frac{(H-h_e)}{L}$ when $m = 1$.

The equation (2.9) can be written in the following dimensionless form.

$$\alpha^m \eta_3^m - 1 = 0 \quad (2.10)$$

where η_3 is the nonlinearity parameter.

Solutions of the equation (2.10), are presented in Figure (6) for d versus η_3 on semilogarithmic plot.

With increasing value of η_3 i.e. increasing nonlinearity, the actual discharge decreases logarithmically. The actual discharge increases with increasing value of m for values of η_3 upto 1.0, when $m = 1$, linear case, the discharge ratio remains same for all values of η_3 . For value of $\eta_3 = 1.0$ the effect of nonlinearity on discharge ratio is nil. For low values of η_3 ($\eta_3 < 1.0$) the actual discharge is higher than linear case discharge and vice versa.

2.2 Flow into a Trench - Gravity Flow

2.2.1 Case (1)

Figure (2) illustrates the problem under consideration.

The average velocity of flow 'V' is given by

$$V = \frac{Q}{B.h} \quad (2.11)$$

where $B.h$ is equal to area of flow.

$$1 = \frac{dh}{dy}$$

Substituting the equation (2.11) in equation (1.2),

$$1 = \frac{aQ}{Bh} + \frac{bQ^2}{B^2 h^2} \quad (2.12)$$

Integrating equation (2.12) with boundary conditions

$y = 0$, $h = h_e$, and $y = L$, $h = H$,

$$\begin{aligned} (h^2 - h_e^2) - A (h - h_e) + A^2 \log_e \left\{ \frac{h + A}{h_e + A} \right\} \\ = \frac{aQ}{B} y \end{aligned} \quad (2.13)$$

where $A = \frac{bQ}{aB}$

$$\begin{aligned} 1 - \eta_1 \alpha + \eta_1^2 \alpha^2 \frac{(1+r_{d1})}{2(1-r_{d1})} \log_e \left\{ \frac{2 + \eta_1 \alpha (1+r_{d1})}{2r_{d1} + \eta_1 \alpha (1+r_{d1})} \right\} \\ = \alpha \end{aligned} \quad (2.14)$$

where drawdown ratio r_{d1} is equal to $\frac{h_e}{H}$ and η_1 is equal to $\frac{b}{a^2} \left(\frac{H - h_e}{L} \right)$

$$\begin{aligned} \frac{(1-Z^2)}{(1-r_{d1}^2)} - \eta_1 \alpha \frac{(1-Z)}{(1-r_{d1})} + \eta_1^2 \alpha^2 \frac{(1+r_{d1})}{2(1-r_{d1})} \times \\ \log_e \left\{ \frac{2 + \eta_1 \alpha (1+r_{d1})}{2Z + \eta_1 \alpha (1+r_{d1})} \right\} \\ = (1 - y/L) \end{aligned} \quad (2.15)$$

where Z is equal to $\frac{h}{H}$

Equations (2.14) and (2.15) can be solved by the method of iteration for calculating values of α and Z respectively.

The solution to the equation (2.14) is represented in the figure (7). It can be seen from the figure (7), that the value of η_1 between .01 and 1.0 discharge ratio decreases logarithmically and discharge ratio increases again for $\eta_1 > 1.0$. Thus the effect of nonlinearity parameter (η_1) may decrease or increase discharge ratio depending on the value of η_1 . For same drawdown discharge is always less for nonlinear flow than that for linear flow. The effect of drawdown ratio (r_{d1}) on discharge ratio is insignificant and for values of $\eta_1 < .10$, it is practically nil.

2.2.2 Variation of Discharge with Drawdown Ratio

The equation (2.13) may also be written in the following form.

For $B = 1$,

$$\frac{H^2}{h_e^2} = 2 \left[(Q_{*2} \frac{L}{h_e} + Q_{*2} \eta_2 (\frac{H}{h_e} - 1) - (Q_{*2} \eta_2)^2 \log_e \left\{ \frac{\frac{H}{h_e} + Q_{*2} \eta_2}{1 + Q_{*2} \eta_2} \right\} \right] + 1.0 \quad (2.16)$$

where Q_{*2} is dimensionless discharge and equals to $\frac{a.q.}{h_e}$.

For $\frac{L}{h_e}$ ratio equals to 20.0, solutions to the equation (2.16) are shown in figure (8) on semilogarithmic paper. The effect of nonlinearity parameter i.e. η_2 on $\frac{H}{h_e}$ ratio for a given value of Q_2 is almost same for all values of η_2 between .01 to .10, and for lower value of η_2 , $\frac{H}{h_e}$ ratio increases more rapidly than for higher values.

2.2.3 Case (11) . Solution by Power Law

Solution to the unconfined trench flow by using equation (1.3)

$$\begin{aligned} u &= CV^m \\ &= \frac{dh}{dy} \\ \frac{dh}{dy} &= C \left(\frac{Q}{Bh} \right)^m \end{aligned} \quad (2.17)$$

Integrating equation (2.17) with boundary conditions at $y = 0$, $h = h_e$ and $y = L$, $h = H$.

$$\frac{H^{m+1} - h_e^{m+1}}{m+1} = C \left(\frac{Q}{B} \right)^m L \quad (2.18)$$

when $m = 1$, $Q = Q_L$, linear case.

with $d = Q/Q_L$

$$\frac{H^{m+1} - h_e^{m+1}}{L^{m+1}} = \frac{\mathcal{L}^m}{C^{m-1}} \left(\frac{H^2 - h_e^2}{2L} \right)^m \quad (2.19)$$

$$\text{For } \frac{H}{h_e} = 2.0$$

$$\text{and } \eta_4 = \frac{CL}{h_e}$$

The equation (2.19) reduces to the following dimensionless form

$$\mathcal{L} = \frac{2}{3} \left[\frac{2^{m+1} - 1}{m+1} \right]^{\frac{1}{m}} \eta_4^{\frac{m-1}{m}} \quad (2.20)$$

The solution of the equation (2.20) is represented in figure (9), by plotting \mathcal{L} versus η_4 on semilogarithmic paper. From the plot it can be seen that discharge ratio increases with increasing value of η_4 and m . For all values of η_4 greater than 1.0, \mathcal{L} is greater than 1.0, i.e. nonlinear discharge is more than linear discharge. When η_4 equals to 1.0, the effect of m on discharge ratio is nil.

2.3. Flow into a trench - Combined Artesian and Gravity Flow

2.3.1 Figure (3) illustrates a trench in a stratum under combined artesian and gravity flow.

Let L_G be the distance from the face of the trench to the point at which flow changes from artesian to gravity

type. For value of y upto L_G , flow is gravity type and for y between L_G and L flow is artesian type.

For artesian flow

$$v = \frac{Q}{BD}$$

Using equation (1.3)

$$\begin{aligned} i &= \frac{dh}{dy} \\ &= C \cdot \left(\frac{Q}{BD} \right)^m \end{aligned} \quad (2.21)$$

Integrating equation (2.21) for boundary conditions at $y = L_G$, $h = D$

$$\frac{h-D}{(y-L_G)} = C \left(\frac{Q}{BD} \right)^m \quad (2.22)$$

At $y = L$, $h = H$

$$C \left(\frac{Q}{BD} \right)^m - \left(\frac{H-D}{L-L_G} \right) = 0 \quad (2.23)$$

with $Q = \mathcal{L} Q_L$

$$\text{when } m = 1, Q_L = BDK \cdot \left(\frac{H-D}{L-L_G} \right) \quad (2.24)$$

Equation (2.23) can be reduced to the following form

$$\mathcal{L}^m \eta^{m-1} - 1 = 0 \quad (2.25)$$

where $\gamma_5 = \left(\frac{H-D}{C(L-L_G)} \right)$

For gravity flow,

$$\gamma = \frac{Q}{h \cdot B}$$

$$1 = \frac{dh}{dy}$$

$$= C \left(\frac{Q}{hB} \right)^m \quad (2.26)$$

Integrating the equation (2.26) for h with boundary conditions at $y = 0$, $h = h_e$ and $y = L_G$, $h = D$.

$$\frac{D^{m+1} - h_e^{m+1}}{m+1} = C \left(\frac{Q}{B} \right)^m L_G \quad (2.27)$$

with $Q = \alpha Q_L$

$$\frac{D^{m+1} - h_e^{m+1}}{m+1} = \frac{1}{C^{m-1}} \alpha^m \cdot \left(\frac{D^2 - h_e^2}{2 L_G} \right)^m \cdot L_G \quad (2.28)$$

The value of discharge (Q) is same in equations (2.25) and (2.27) by continuity.

Distance L_G at which flow changes from gravity to artesian type is found out from equations (2.23) and (2.27).

Equating the equations (2.23) and (2.27) for the value of Q.

$$\frac{H-D}{(L-L_G)} = \frac{D}{L_G} \frac{(1-r_{d2}^{m+1})}{(n+1)} \quad (2.29)$$

where $r_{d2} = \frac{h_e}{D}$

$$\frac{L_G}{L} = \frac{D(1-r_{d2}^{m+1})}{(H-D)(m+1) + D(1-r_{d2}^{m+1})} \quad (2.30)$$

For $\frac{H}{D} = 2.0$, equation (2.30) simplifies to

$$\frac{L_G}{L} = \frac{(1-r_{d2}^{m+1})}{(m+2 - r_{d2}^{m+1})} \quad (2.31)$$

when $m = 1$,

$$\frac{L_G}{L} = \frac{(D^2 - h_e^2)}{(2DH - D^2 - h_e^2)} \quad (2.32)$$

i.e. same as linear case.

The equation (2.31) is represented in figure (10) with values of $\frac{L_G}{L}$ versus m . The ratio $\frac{L_G}{L}$ decreases with

increasing values of μ . The effect is more at low values of r_{d2} i.e. upto 0.25. For value of $r_{d2} > 0.75$ the effect of μ on $\frac{L_G}{L}$ ratio is insignificant.

2.4 Radial Flow Into a Well Completely Penetrating a Confined Aquifer (Artesian Flow)

2.4.1 Case (1) :

The problem under consideration is one of radial symmetry and is illustrated in figure (11). The flow is assumed to be two dimensional and ~~a~~ aquifer is homogenous and isotropic. The area of flow at a distance r from the center of the well is $2\pi rD$, where D is the thickness of aquifer.

$$\begin{aligned} V &= \frac{Q}{2\pi rD} \\ u &= \frac{dh}{dr} \\ &= \frac{aQ}{2\pi rD} + \frac{bQ^2}{4\pi^2 r^2 D^2} \end{aligned} \quad (2.37)$$

since at $r = r_w$, $h = h_e$

$$h = h_e + \frac{aQ}{2\pi D} \log_e \left(\frac{r}{r_w} \right) + \frac{bQ^2}{4\pi^2 D^2} \left(\frac{1}{r_w} - \frac{1}{r} \right)$$

$$\text{at } r = R, h = H \quad (2.34)$$

$$H = h_e + \frac{aQ}{2\pi D} \log_e \left(\frac{R}{r_w} \right) + \frac{bQ^2}{4\pi^2 D^2} \left(\frac{1}{r} - \frac{1}{R} \right) \quad (2.35)$$

The discharge ratio $\mathcal{L} = Q/Q_L$ is obtained from

$$\eta_6 \mathcal{L}^2 \frac{(r_{d3} - 1)}{\log_e (r_{d3})^2} + \mathcal{L} - 1 = 0 \quad (2.36)$$

where $\frac{R}{r_w} = r_{d3}$ and $\eta_6 = \frac{b}{a^2} \left(\frac{H-h_e}{R} \right)$

The drawdown curve can be expressed as

$$\frac{h - h_e}{H - h_e} = \frac{\mathcal{L} \log_e (r/r_w)}{\log_e (r_{d3})} + \frac{(1-\mathcal{L})}{(r_{d3}-1)} r_{d3} \times \frac{(r-1)}{r} \quad (2.37)$$

The discharge ratio calculated from equations (2.36) is plotted as \mathcal{L} versus η_6 on semilogarithmic paper in figure (13), with r_{d3} ratio of radii of the third parameter. This discharge ratio (\mathcal{L}) in this case also decreases logarithmically with increasing value. The reduction in \mathcal{L} is more for the range of η_6 between 0.1 and 1.0 than 1.0 to 10.0. Increasing r_{d3} value also have decreasing effect on \mathcal{L} . However for a tenfold increase in r_{d3} , the value of \mathcal{L} decreases by about 0.1, and r_{d3} above 100, the decrease in \mathcal{L} is further reduced.

2.4.2 Case (11) - Power Law Solution

In this case, solution to the above problem is obtained by equation (1.3)

$$u = CV^m$$

$$= \frac{dh}{dr}$$

$$V = \frac{Q}{2 \pi r D}$$

At $r = r_w$, $h = h_e$

$$h - h_e = C \left(\frac{Q}{2 \pi D} \right)^m \left[\frac{1}{(1-m) r^{m-1}} - \frac{1}{(1-m) r_w^{m-1}} \right] \quad (2.38)$$

At $r = R$, $h = H$.

$$H - h_e = C \left(\frac{Q}{2 \pi D} \right)^m \left[\frac{1}{(1-m) R^{m-1}} - \frac{1}{(1-m) r_w^{m-1}} \right] \quad (2.39)$$

The discharge ratio $\mathcal{L} = Q/Q_L$ is obtained from

$$\begin{aligned} \mathcal{L} &= \left(\frac{H - h_e}{H - h_e} \right)^{\frac{m-1}{m}} \left(R^{m-1} - r_w^{m-1} \right)^{\frac{1}{m}} \log_e \left(\frac{R}{r_w} \right) \\ &= \eta_7 \frac{m-1}{m} \left\{ \left(1 - \left(\frac{1}{r_{d3}} \right)^{m-1} \right) \right\}^{\frac{1}{m}} \log_e r_{d3} \end{aligned} \quad (2.40)$$

where $\eta_7 = \frac{CR}{(H-h_e)}$

and $r_{d3} = \frac{R}{r_w}$

The solution to the equation - represented in figure (14) for \mathcal{L} as function of η_7 . The increasing values of η_7 and r_{d3} increases the discharge ratio (\mathcal{L}) logarithmically and maximum discharge rate for a given value of η_7 and r_{d3} occurs when $m = 2.0$. The discharge ratio increases considerably for η_7 between 1.0 and 10.0 than for lower values.

2.5.1 Radial Flow Into a Well Completely Penetrating an Unconfined Aquifer (Gravity Flow)

Case (1)

An equation for steady radial flow to a well in an unconfined aquifer using Forchheimer's equation (1.2). Referring to the figure (12)

$$\frac{dh}{dr} = \frac{Q \cdot a}{2\pi r h} + \frac{Q^2}{4\pi^2 r^2 h^2} \quad b \quad (2.41)$$

where $2\pi r h$ is the area of flow at distance r from the

center of the well.

$$r^2 h^2 \frac{dh}{dr} - \frac{aQ}{2\pi} rh - \frac{bQ^2}{4\pi^2} = 0 \quad (2.42)$$

$$\text{Let } \frac{r}{r_w} = R_1$$

$$\frac{h}{h_e} = H_1$$

$$\frac{dh}{dr} = \frac{h_e}{r_w} \frac{dH_1}{dR_1} \quad (2.43)$$

Substituting equation (2.43) in (2.42)

$$\frac{dH_1}{dR_1} = \frac{1}{R_1 \times H_1} \frac{aQ}{2\pi h_e^2} + \frac{bQ^2}{4\pi^2 (r_w \cdot h_e^3)} \frac{1}{H_1^2 \times R_1^2} \quad (2.44)$$

If $Q_* = \frac{Q \cdot a}{\pi h_e^2}$ (dimensionless discharge) and

$$\frac{r_w}{h_e} = r_{d4},$$

$$\frac{dH_1}{dR_1} = \frac{Q_*}{2R_1 \times H_1} + \frac{Q_*^2}{4} \gamma_2 \cdot \frac{1}{r_{d4}} \cdot \frac{1}{R_1^2 \times H_1^2} \quad (2.45)$$

For linear case equation can be written in the following form

$$\frac{h}{h_e} = \sqrt{Q_{d*} \cdot \log_e \left(\frac{r}{r_w} \right) + 1.0} \quad (2.46)$$

and Q_{d*} is dimensionless linear discharge and is equal to $\frac{Q_L}{h_e^2 \pi K}$.

The solution to the equation (2.45) is represented in figures (15) (16) (17) and (18). Since the exact solution is not possible for the equation (2.45), numerical solution was obtained by Runge-Kutta method, with the aid of digital computer facility.

In the figure (15) the ratio $\frac{h}{h_e}$ is plotted against $\frac{r}{r_w}$ for different values of Q_* , keeping parameter η_2 and r_{d4} constant. The solution to the equation (2.46) is also represented in this figure for comparing linear and non-linear flows. For the same discharge (dimensionless) Q_* and Q_{d*} the effect of nonlinearity increases the drawdown ratio $\left(\frac{h}{h_e}\right)$. For linear case increase in $\frac{h}{h_e}$ value is gradual. For example for the discharge $Q_{d*} = 0.1$, for increase in $\frac{r}{r_w}$ value from 1.0 to 10.0, drawdown ratio increases by about 10% for linear case whereas for nonlinear case, drawdown ratio increases by about 10 times its initial value.

In the figure (16), $\frac{h}{h_e}$ versus $\frac{r}{r_w}$ is represented for same range of Q_x , with higher values of η_2 i.e. nonlinearity parameter. In this case also the plot is similar to previous case. However at lower value of $\frac{r}{r_w}$ between 1.0 and 3.0, effect of nonlinearity parameter (η_2) on $\frac{h}{h_e}$ ratio is pronounced.

Figure (17) shows the plot of $\frac{h}{h_e}$ versus $\frac{r}{r_w}$ for values of η_2 ranging from 0.001 to 100.0 for some value of Q_x . The effect of nonlinearity parameter (η_2) on drawdown ratio $\frac{h}{h_e}$ is insignificant for value of η_2 upto 10.0. For η_2 equals to 100, drawdown ratio increases by about .05.

Figure (18) shows the plot of $\frac{h}{h_e}$ versus $\frac{r}{r_w}$ for varying values of r_{d4} , keeping η_2 and Q_x constant. From the figure (18) it is evident that r_{d4} value has no effect on drawdown ratio, since for all values of r_{d4} drawdown ratio is represented by single curve.

2.5.2 Case (11) : Power Law Solution

From equation (1.3),

$$\begin{aligned} \frac{dh}{dr} &= CV^m \\ &= C \left(\frac{Q}{2\pi rh} \right)^m \end{aligned} \quad (2.47)$$

Integrating the equation (2.46) for h with boundary

conditions, the following equation (2.48) can be obtained.

$$Q^m = \frac{1}{C} \frac{(1-m)(2\pi)^m}{(1+m)} \frac{(H^{1+m} - h_e^{1+m})}{(R^{1-m} - r_w^{1-m})} \quad (2.48)$$

when $m = 1$, $Q = Q_L$ linear case.

With $C = \mathcal{L} Q_L$ and $r_{d3} = \frac{R}{r_w}$, the equation (2.48) may be reduced to the following form.

$$\mathcal{L} = \left(\frac{\mathcal{L}}{3} \right) \left\{ \frac{(1-m)}{(1+m)} \left[\frac{\left(\frac{H}{h_e} \right)^{1+m} - 1}{r_{d3}^{1-m} - 1} \right] \right\}^{\frac{1}{m}} \eta_8^{\frac{m-1}{m}} \log_e r_{d3} \quad (2.49)$$

where $\eta_8 = \frac{r_w C}{h_e}$

The solution of the equation (2.49) is shown in figure (19), for \mathcal{L} as function of η_8 with m as third parameter. For values of m upto 1.2, increase in \mathcal{L} for all values of η_8 is gradual i.e. \mathcal{L} versus η_8 relationship is almost a straight line. For all values of r_{d3} and η_8 less than 0.10, variation in \mathcal{L} is insignificant and \mathcal{L} increases with increase in the value of m .

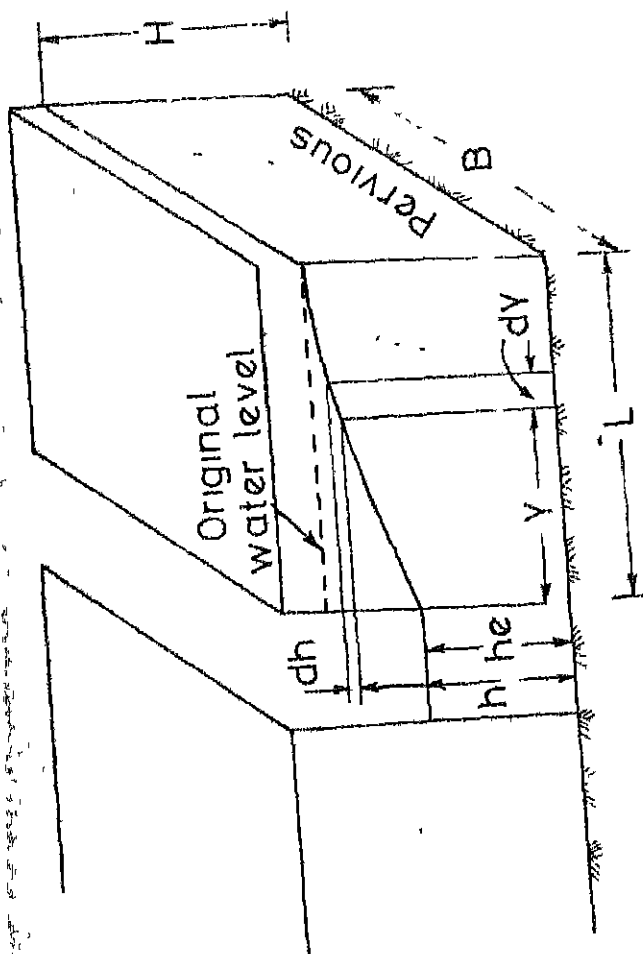


FIG.2 UNCONFINED TRENCH FLOW

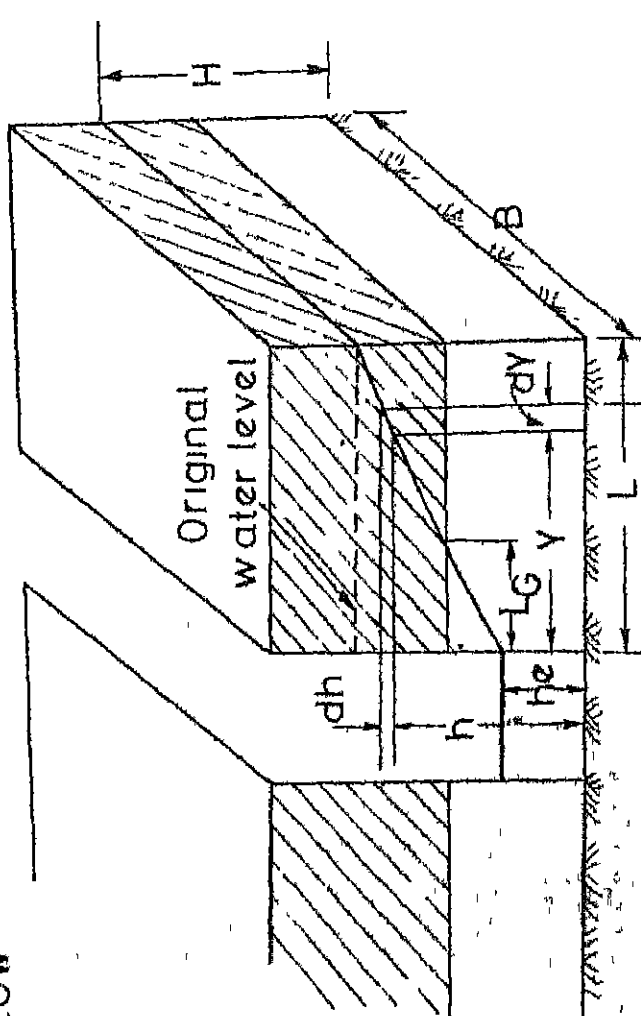


FIG.3 CONFINED - UNCONFINED TRENCH FLOW

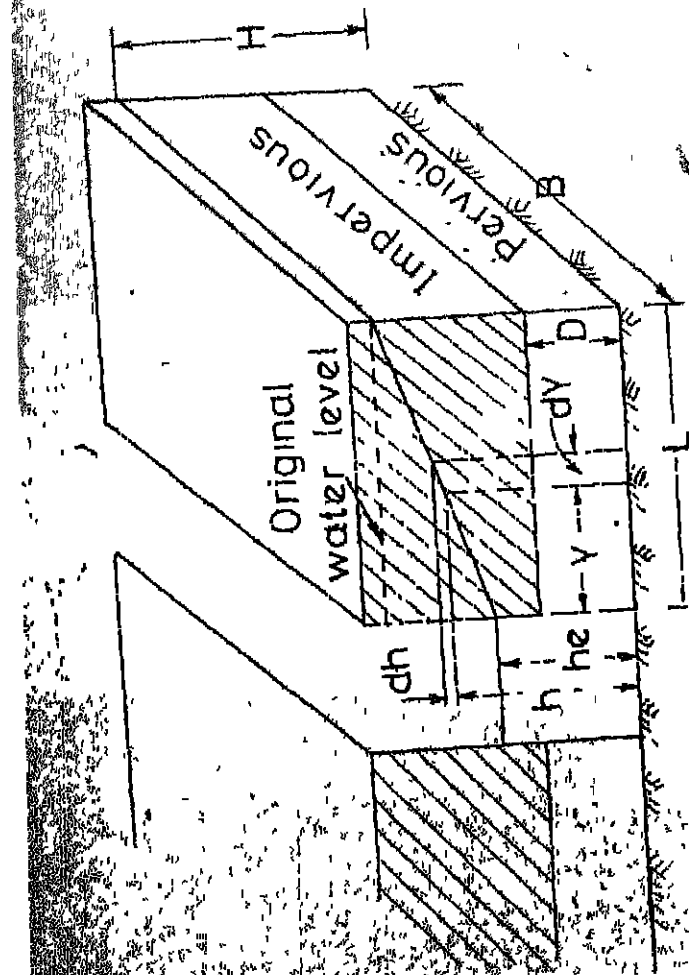


FIG.1 CONFINED TRENCH FLOW

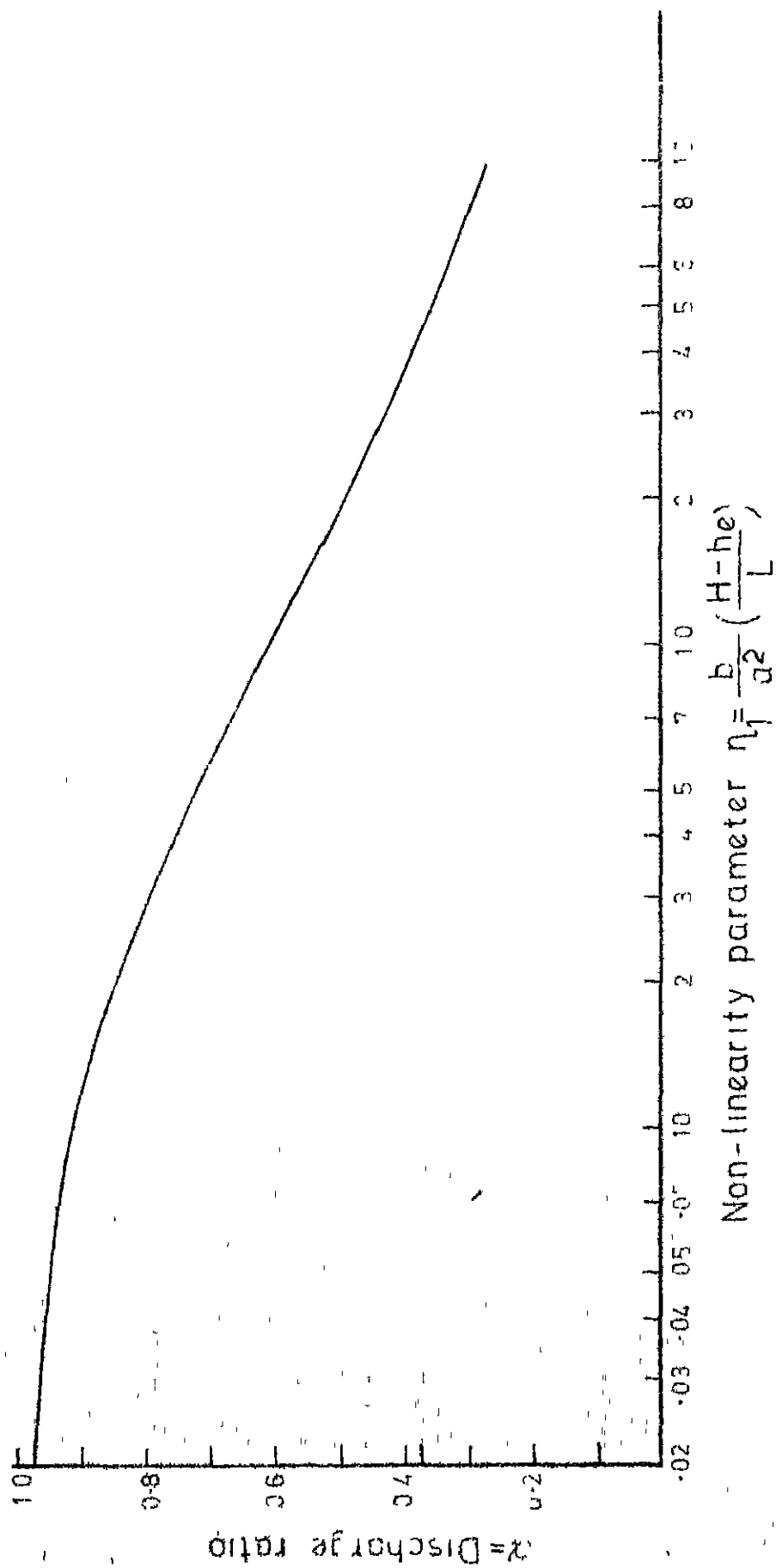


FIG. 4 CONFINED TRENCH FLOW (ARTESIAN FLOW)
(FORCHHEIMERS EQN)

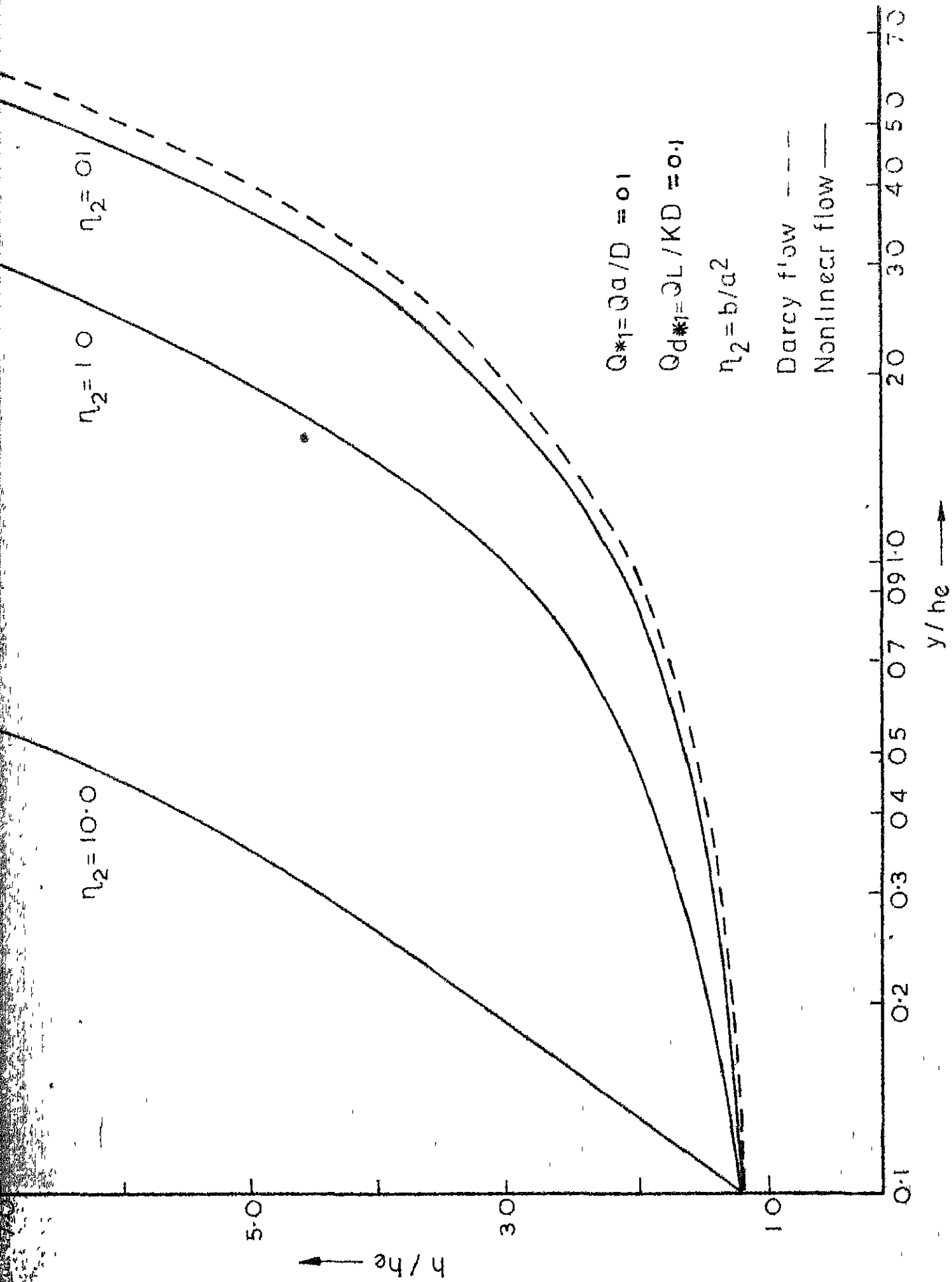
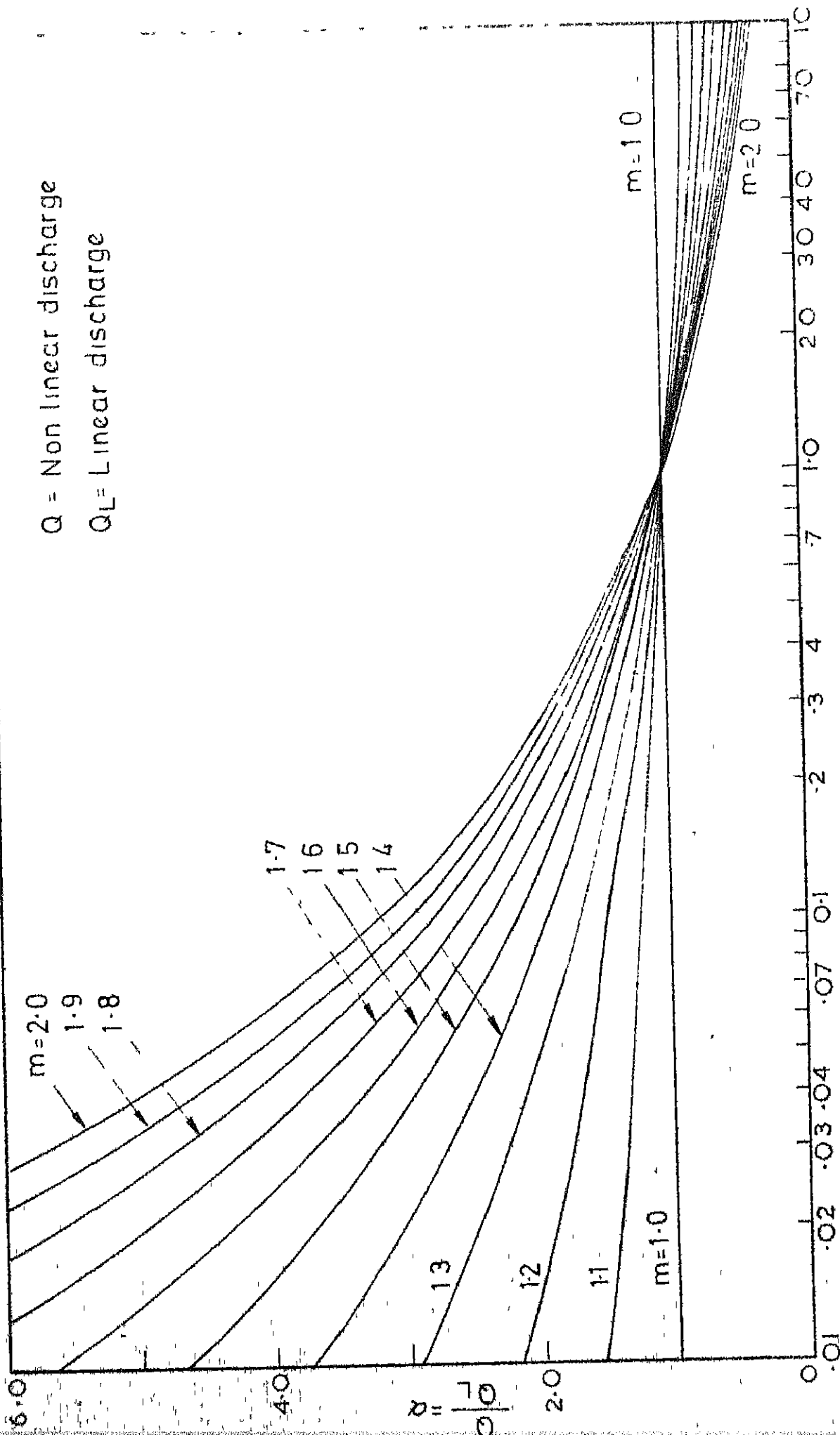


FIG. 5. CONFINED TRENCH FLOW (FORCING FUNCTION)

Q = Non linear discharge
 Q_L = Linear discharge



$$Q_3 = \frac{H - h_e}{LC}$$

FIG. 6. CONFINED TRENCH FLOW (POWER LAW)

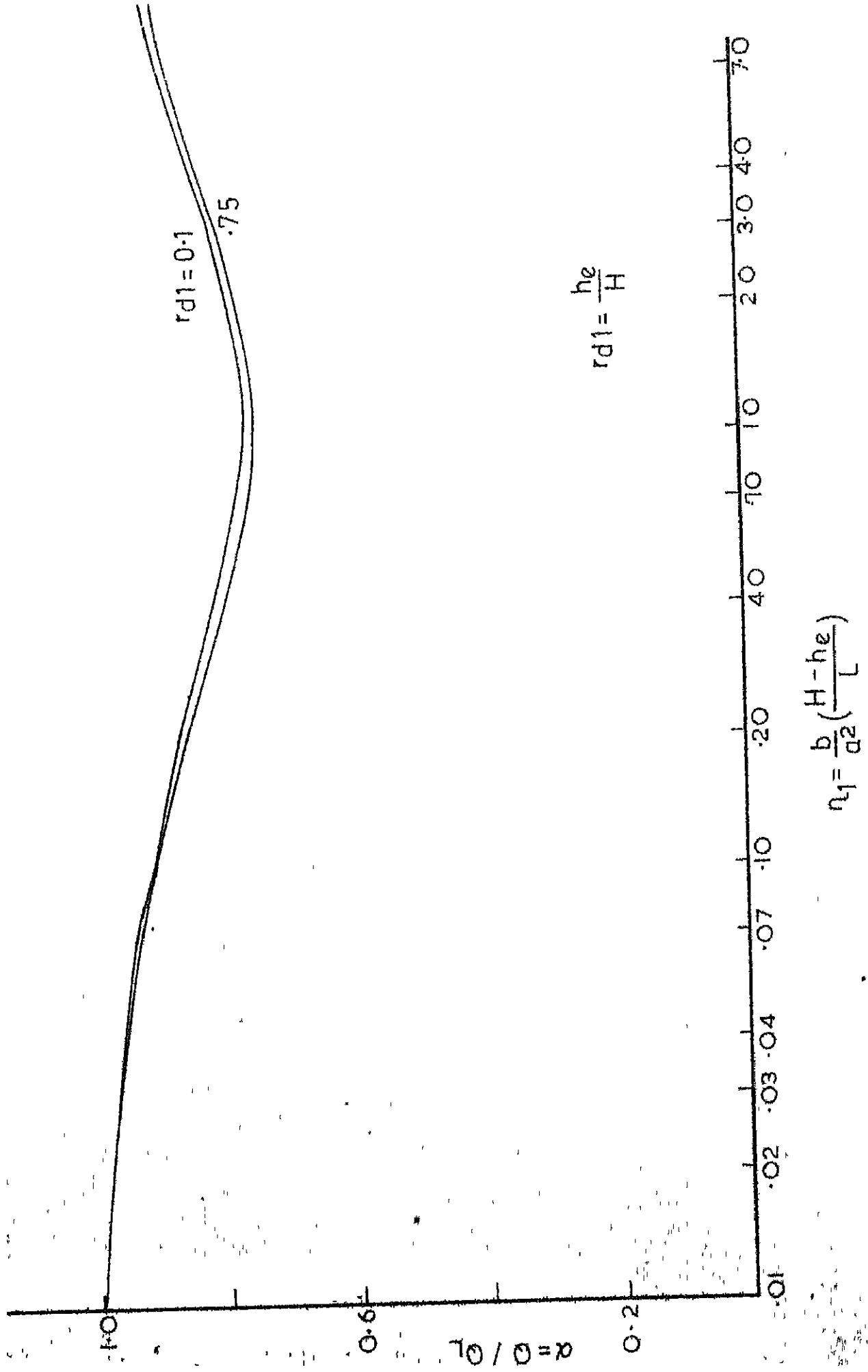


FIG.7 UNCONFINED TRENCH FLOW (FORCHHEIMER'S EQN)

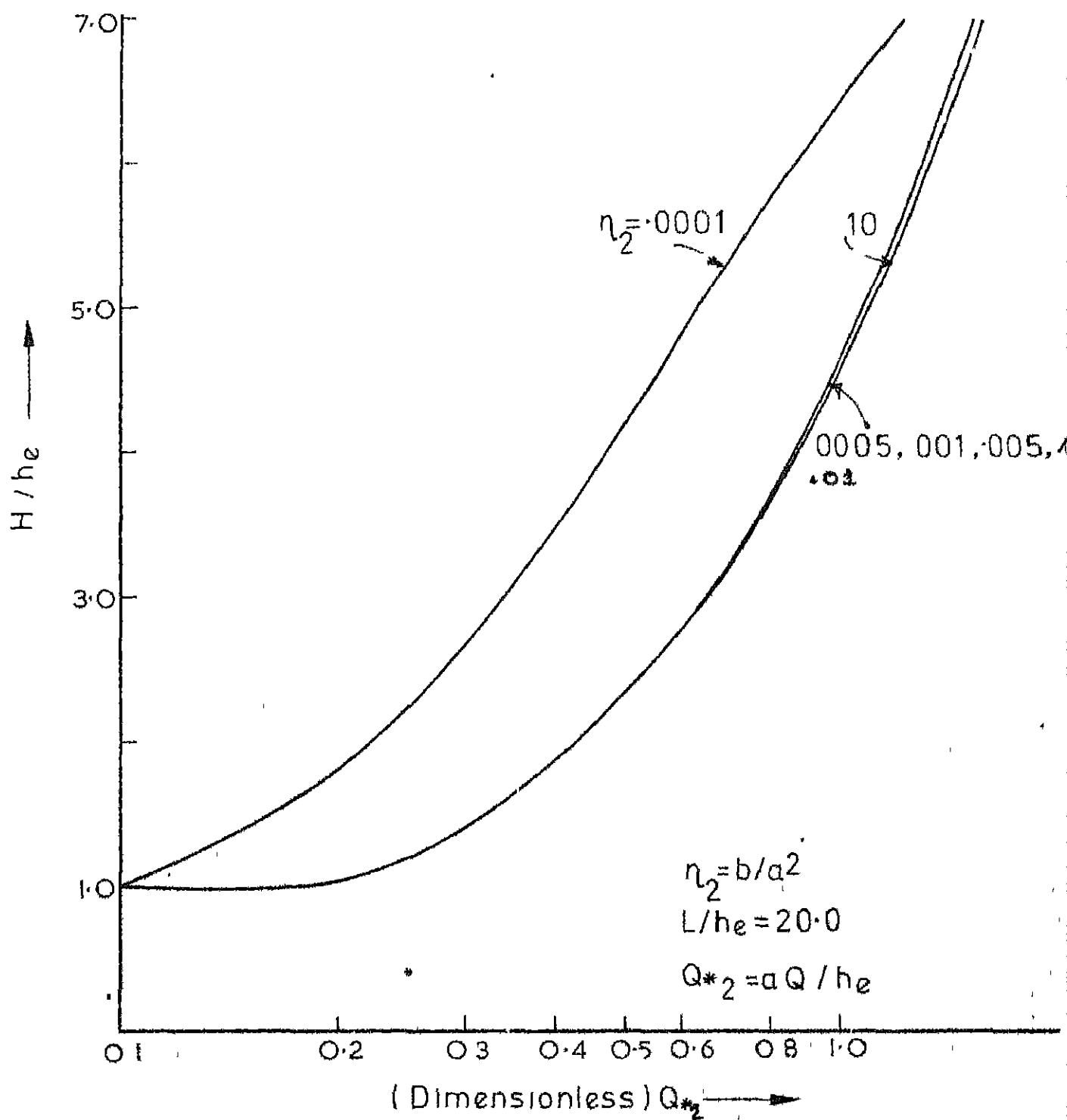
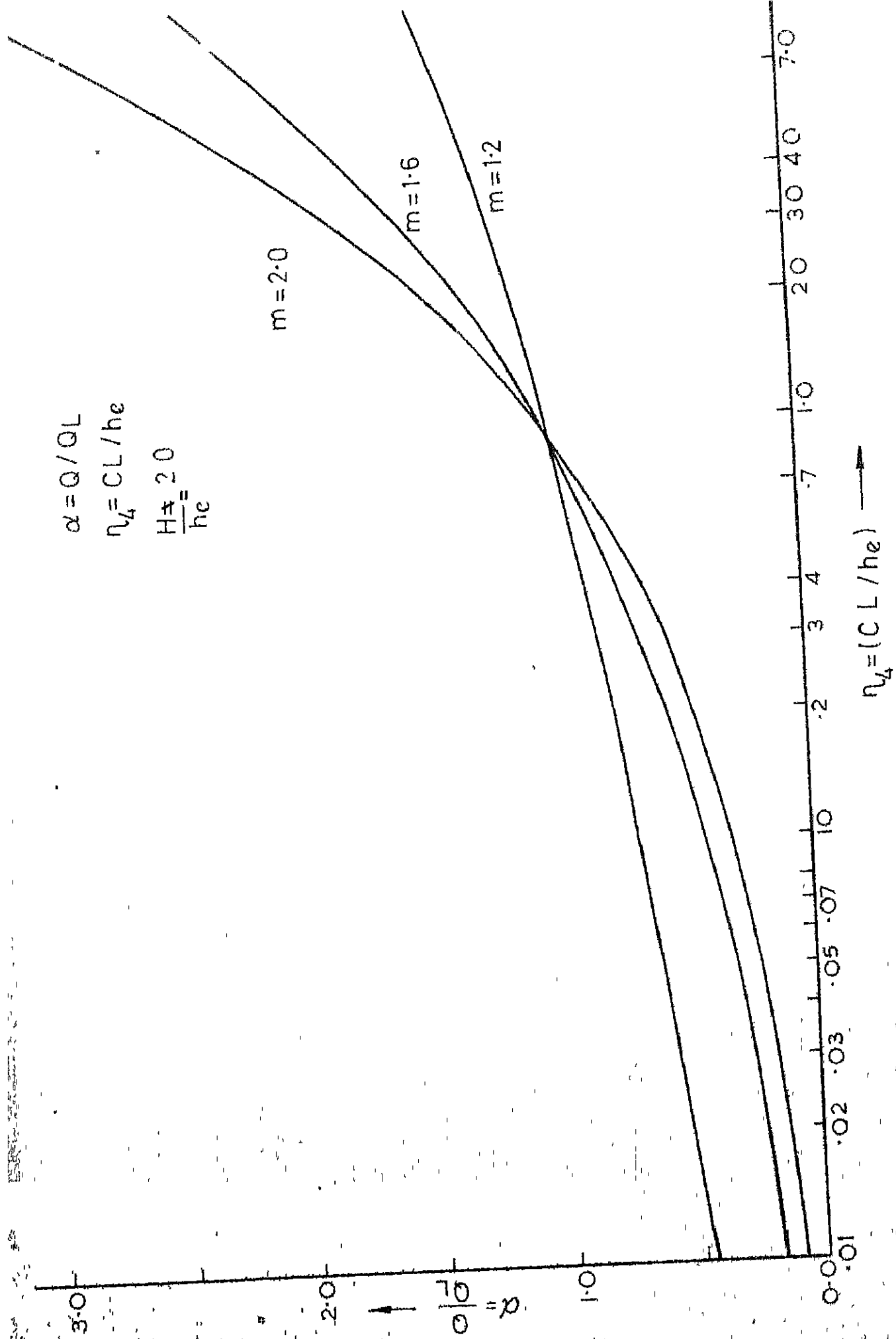


FIG. 8. UNCONFINED TRENCH FLOW (FORCHHEIMER EQN.)



UNCONFINED TRENCH FLOW (POWER LAW)

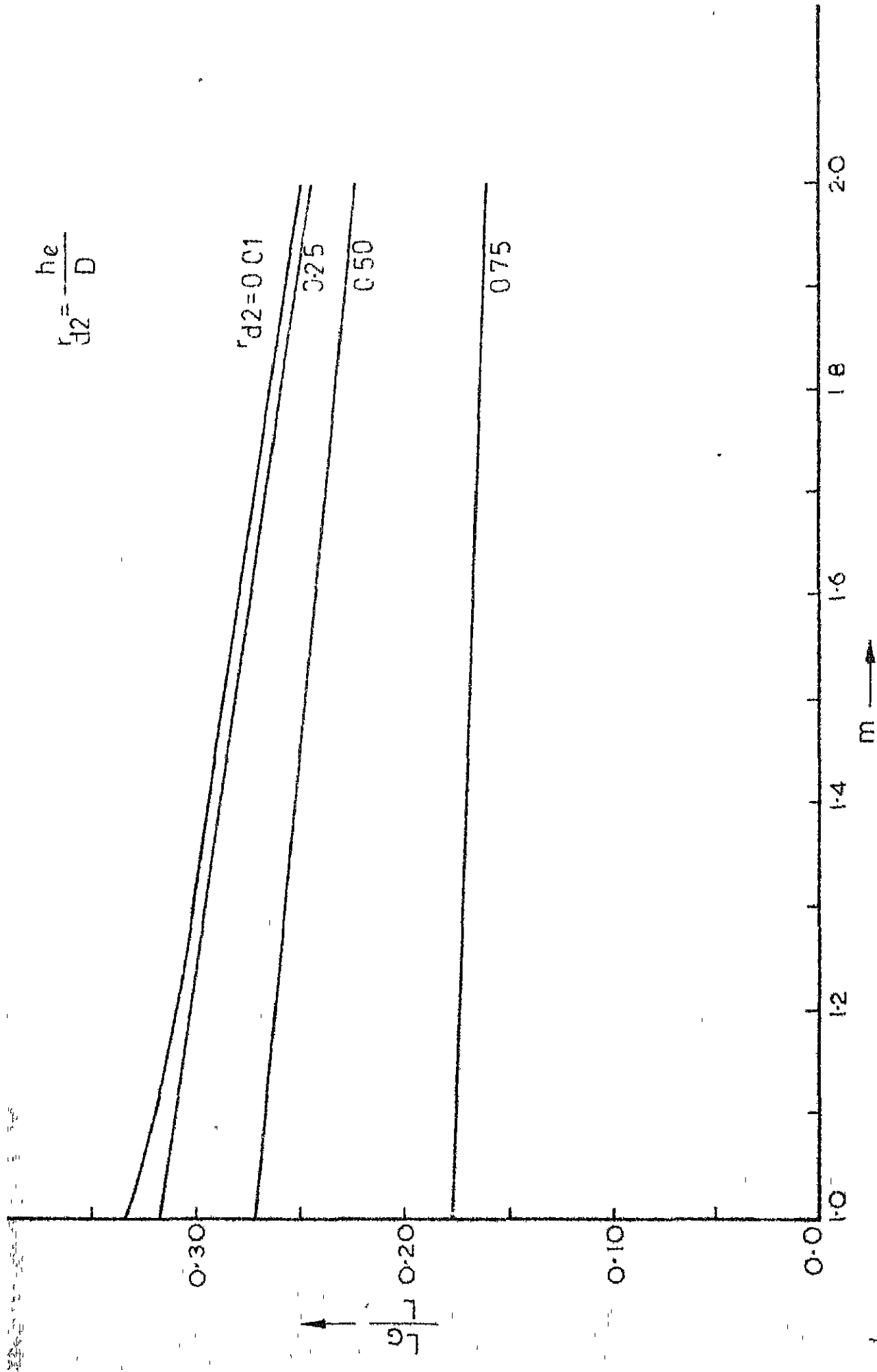


FIG. 10 COMBINED ARTESIAN-GRAVITY TRENCH FLOW (POWER LAW)

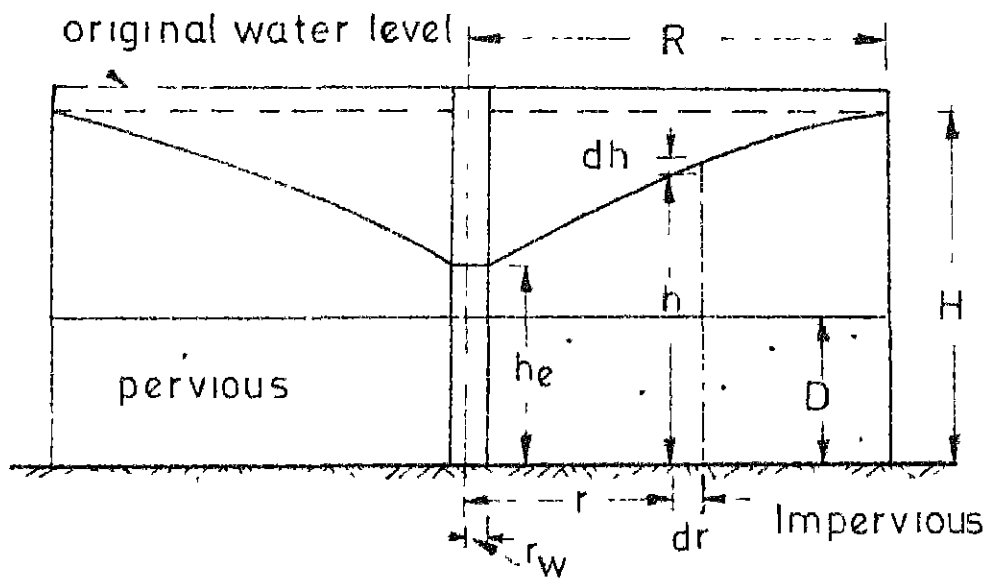


FIG II ARTESIAN WELL FLOW (CONFINED)

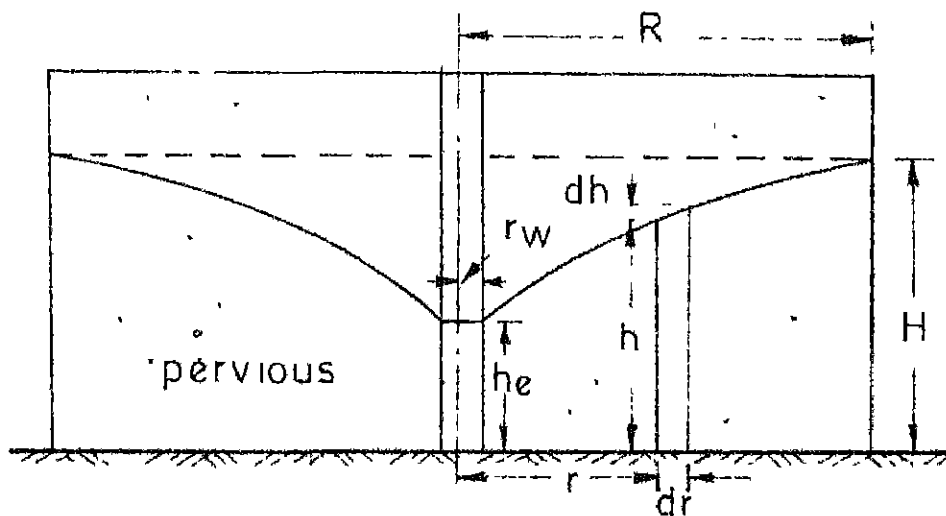


FIG.12 GRAVITY WELL FLOW (UNCONFINED)

DEFINITION SKETCH

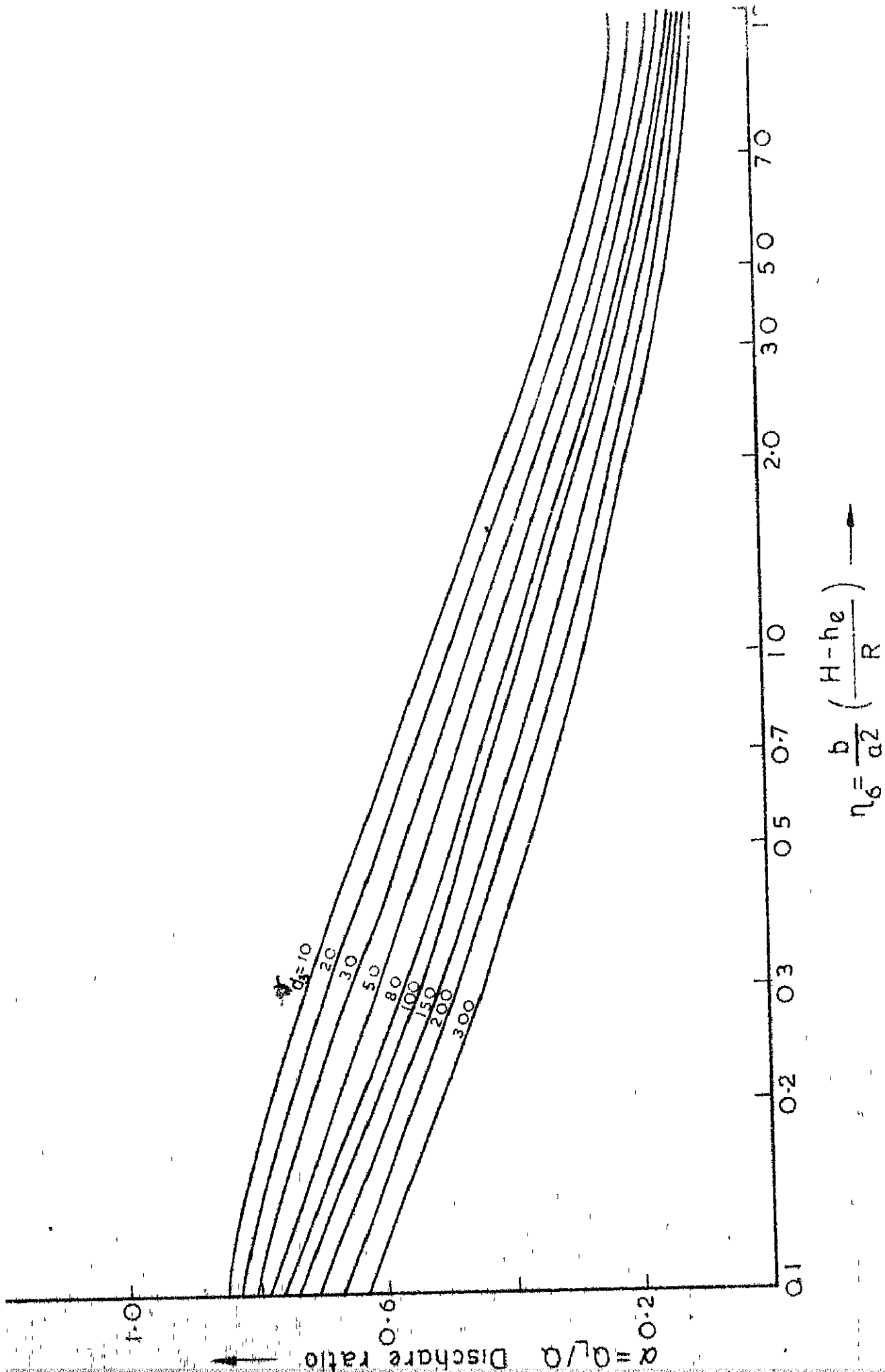


FIG. 13. ARTESIAN WELL FLOW (FORCHHEIMERS EQN.)

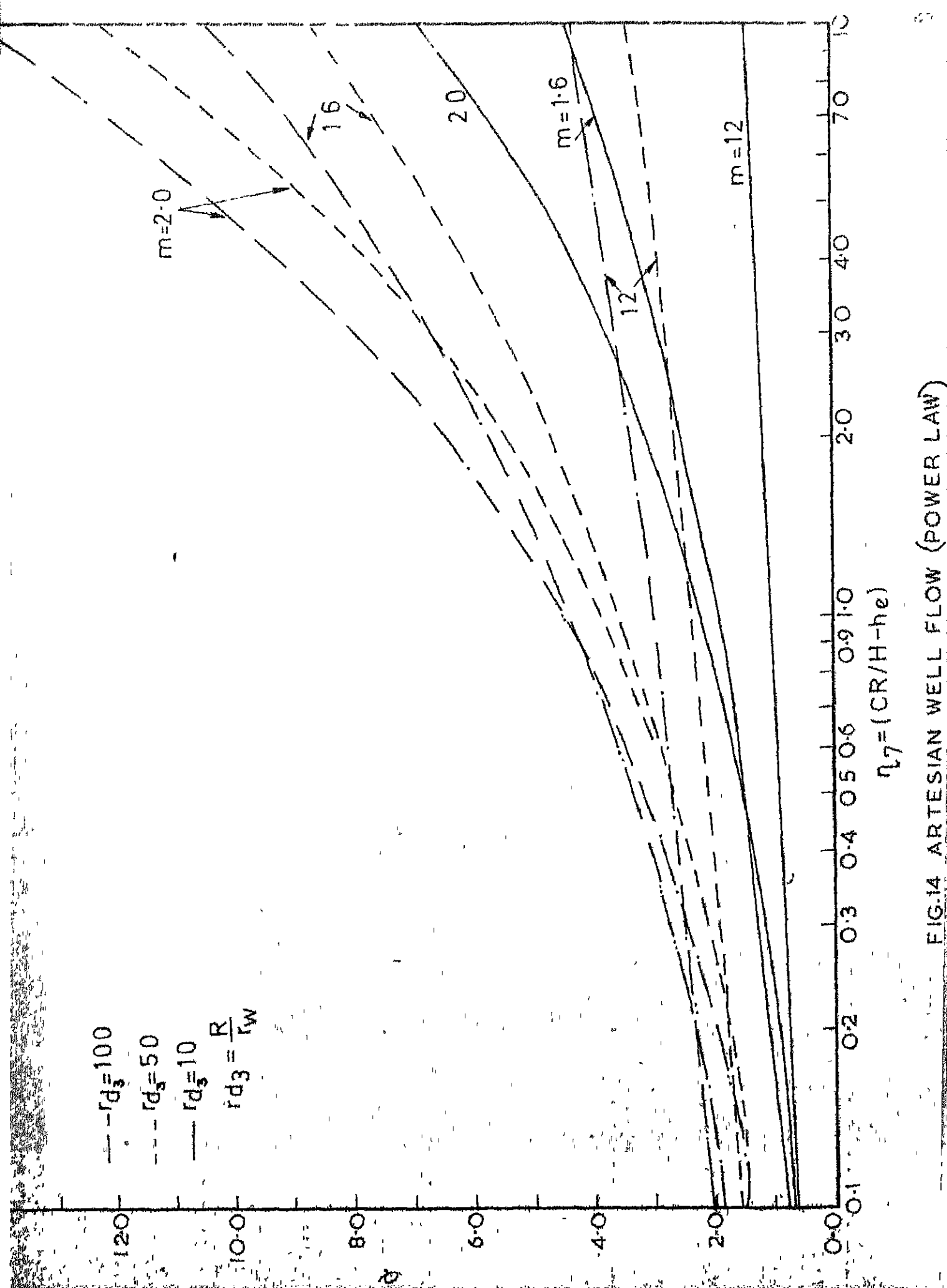


FIG.14 ARTESIAN WELL FLOW (POWER LAW)

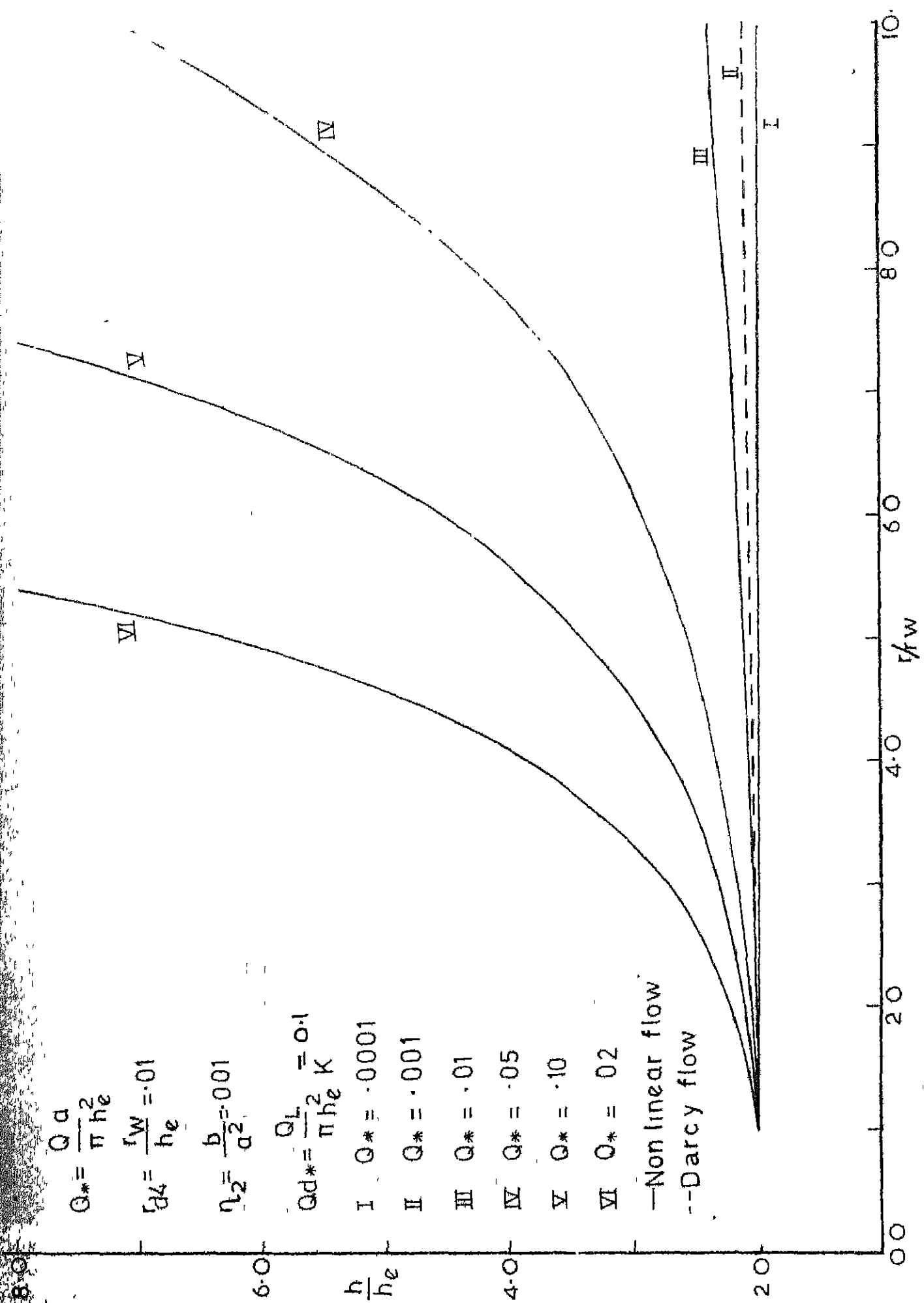


FIG.15 UNCONFINED WELL FLOW (FORCHELMEPS FOR)

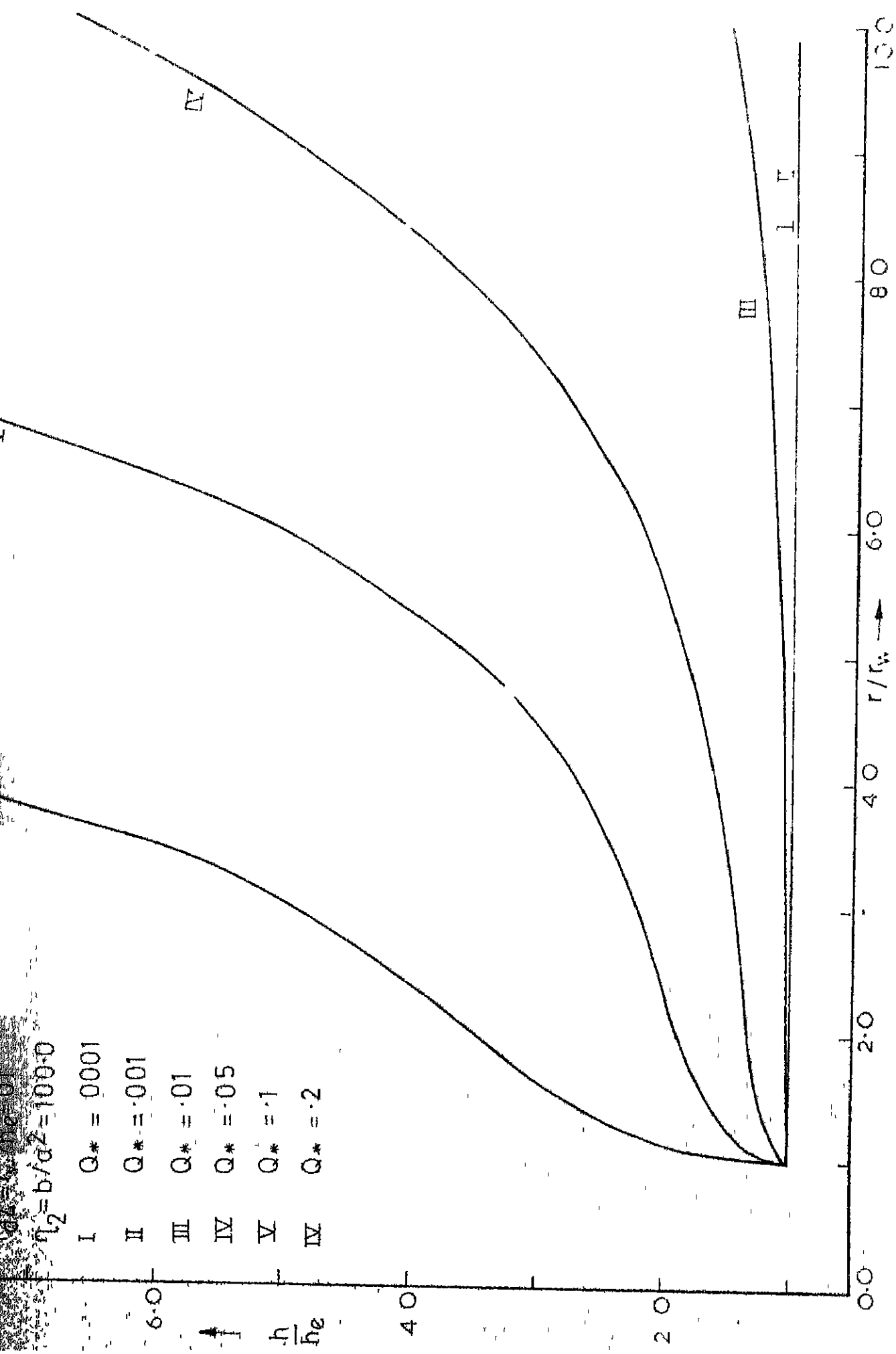


FIG 16 UNCONFINED WELL FLOW

$$Q_* = \frac{Qa}{\pi h_e^2} = 0.1$$

$$\eta_2 = \frac{b}{a^2}$$

$$r_{d4} = \frac{r_w}{h_e} = 0.1$$

h/h_e

1000

VI

I, II, III, IV, V

$\eta_2 = 0.01, 0.1, 1, 1.0, 10.0$

0.0

2.0

4.0

6.0

8.0

10.0

r/r_w

FIG 17 UNCONFINED WELL FLOW (FORCHHEIMER'S EQN)

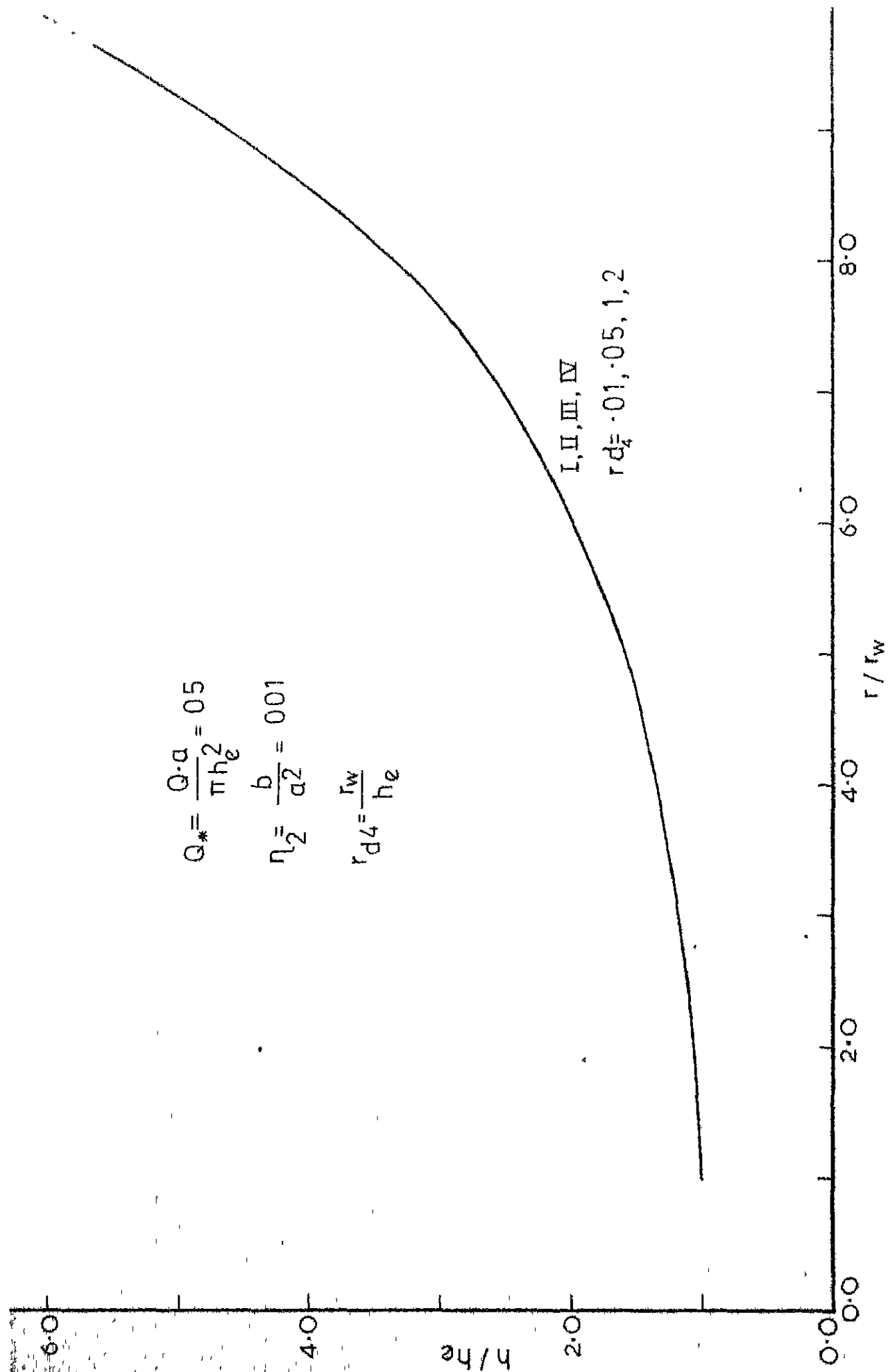


FIG. 18 UNCONFINED WELL FLOW (FORCHHEIMER'S EQN)

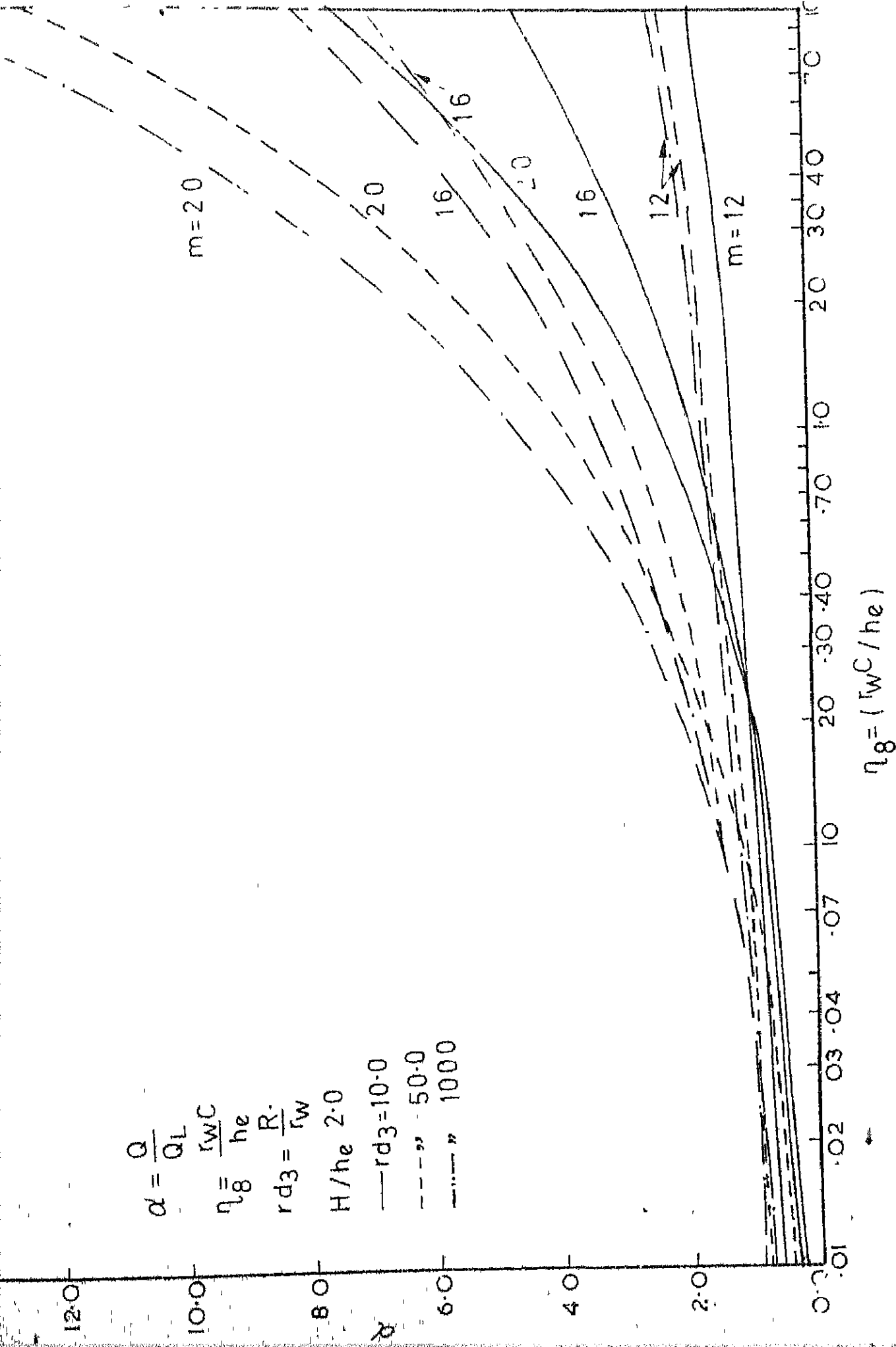


FIG 19 UNCONFINED WELL FLOW (POWER LAW)

CHAPTER III

STUDY OF NON-LINEAR FLOW

3.1 Purpose of the Experiment

This investigation deals with the study of flow of water through porous media and specifically the coefficients in the Forchheimers equation.

3.2 Experimental Set-up

A Schematic diagram of the experimental arrangement is shown in figure (20). A continuous flow supply was provided by a overhead tank which maintains constant head. The permeameter was 15 cms diameter tube and 37.5 cms in length with number of pressure tapplings along the length of the tube. To prevent the channeling along the cylinder walls, the pressure taps were placed in the permeameter so that each tap was 90° around the cylinder from the tap below. A thin metal plate with perforations was placed below the permeameter to support the material filled in the test section. The details of the permeameter tube is shown in the figure (21). The permeameter tube was connected to a long pipe, 15 cms in diameter, which in turn was connected to the

overhead tank. A valve provided at the junction connecting the vertical pipe section to the long pipe at the ground level, controls the flow rate through the permeameter. The water flows through the permeameter vertically downwards. A valve provided at the downstream end of the permeameters connects the 15 cms pipe with a 7.5 cms diameter pipe which rests inside the measuring tank. The measuring tank, 90 cms x 75 cms, which collects the water at the exit end of the pipe was provided with a 90° V-notch to measure the discharge. A drain adjacent to the measuring tank collects the water which in turn flows to a sump and a centrifugal pump lifts the water to the overhead tank to complete the cycle. Pressure head at various tappings were measured with a mercury manometer. Another manometer was used to check the measurements.

3.3 Procedure

Materials - In this investigation 3 types of materials were used, namely river gravel, granite gravel and glass spheres. The physical properties of these materials are given in the table (5).

For the studies of river gravel the permeameter was filled with the river gravel of median diameter (d₅₀)

0.44 cms, Figure (22) to a height of 50 cms without compacting the material. The density was maintained uniform by placing the material at constant height. A screen (No. 54) was placed on the perforated metal plate and also at the tapping points to prevent choking. The permeameter was properly fixed to the supply pipe and joints were filled with white lead to prevent leakage. Valves at the upstream end and at the downstream end were opened and water was allowed to flow through the medium. The material was thoroughly saturated and air bubbles at the end of the tappings were carefully removed. The pressure head at various tappings were measured with a mercury manometer.

After calibrating the V-notch, discharge through V-notch was measured with the aid of a point gauge. The temperature during experiment was noted. The procedure was repeated for various heads and corresponding variables were measured. For river gravel the experiment was repeated for 6 runs with different porosities.

The granite gravel used in the experiment were of two sizes; of median diameters (d 50) .547 cms and .318 cms with porosities .45 and .465 respectively.

In the run number 9, glass spheres of 1.5 cms diameter were used as a medium. It was filled to a height of 30 cms as before and permeameter was thoroughly vibrated using a vibrator to keep the porosity of the material uniform.

A total of 7 runs with different materials for various values of porosities were conducted and the summary of the experimental data are given in tables (5) and (6).

5.4 Results and Discussions

The figure (23) represents the plot of $\frac{1}{V}$ versus V for different runs. There exists a straight line relationship for this plot and values of coefficients were obtained from this plot. The table (5) shows the values of a and b obtained for 9 runs for different materials.

Fig. (24) shows the plot of friction factor (F) versus Reynolds number (Re) for different runs. In the same figure two typical curves one for river gravel (X_1) and another for river sand (X_2) are also shown. The curves (X_1) and (X_2) are for Dudgeons data (Lee-1968). It is interesting to note that the experimental curves lies between the two curves (X_1) and (X_2) for measured Reynolds number (Re) upto 1500. For higher Reynolds number (Re) range measured the experimental curve is slightly shifted downwards.

Thus from the relationship between friction factor (F) and Reynolds number (R_e) it can be concluded for Reynolds number range 10-2000. Forchheimers equation is valid.

$$\text{Specific permeability, } k = K \frac{\mu}{\gamma}$$

where K = Darcy's coefficient of permeability

μ = Dynamic viscosity

γ = Specific weight of fluid

The specific permeability (k) is used while correlating a and b values.

The plot of specific permeability k versus coefficient a is shown in figure (25) for the reported data. It is interesting to note a very good correlation exists between the values of k and 'a' and the slope of the line is 45°. The relationship between k and a may be written in the following equation as

$$ak = 10^{-5} \quad (3.1)$$

The values of 'a' obtained in the present studies were plotted against k in Fig. (26). A straight line correlation on a log-log plot is seen. The range of Reynolds number 200-1500. However when the line (X_3) of figure (25) was plotted on this figure (26), it is seen that the line (X_3) is shifted to the right. This can be attributed as the effect of Reynolds number (R_e).

Thus it can be concluded that a and k , and the proportionality constant is a function of Reynolds number (R_0). The good correlation of Figure (25), can be used to predict the coefficient a for known k if the Reynolds number is in the range 10-200.

Figure (27) shows the plot of specific permeability k versus b for the reported data. In this case also a good correlation exists between the values of k and b . The relationship between k and b is given by the equation of the form

$$bk^{0.7} = 1.42 \times 10^{-4} \quad (32)$$

The values of ' b ' obtained in the present studies were plotted against k in Figure (28). A straight line correlation on a log-log plot is seen. The range of Reynolds number 200-1500. However when the line (X_4) of figure (27) was plotted on this figure (28), is seen that the line (X_4) is shifted to the right. This can be attributed as the effect of Reynolds number (R_e).

Thus it can be concluded that b and k and proportionality constant is a function of Reynolds number (R_e). The good correlation between k and b , Figure (27), can be used to predict the coefficient b for known k if the Reynolds number is in the range 10-200.

Prediction of Values a and b :

For a known nearly uniform particle size, the specific permeability is a function of particle size and the variation is shown in figure (29). Hence using Figure (29) (Karrer - 1969), along with the figures (25) and (27), the coefficients a and b in non-linear flow through a granular material of Reynolds number (R_e) range 10-200 can be predicted.

Example - For a particle size of 5 m.m. from the plot of specific permeability versus particle size, Figure (29), specific permeability value is $2 \times 10^{-4} \text{ cms}^2$. The value of a and b can be obtained from the relationship of k versus a and k versus b, Figures (25) and (27). For particle size of 5 m.m. and specific permeability $2 \times 10^{-4} \text{ cms}^2$ the values of a and b are .05 and .041 respectively.

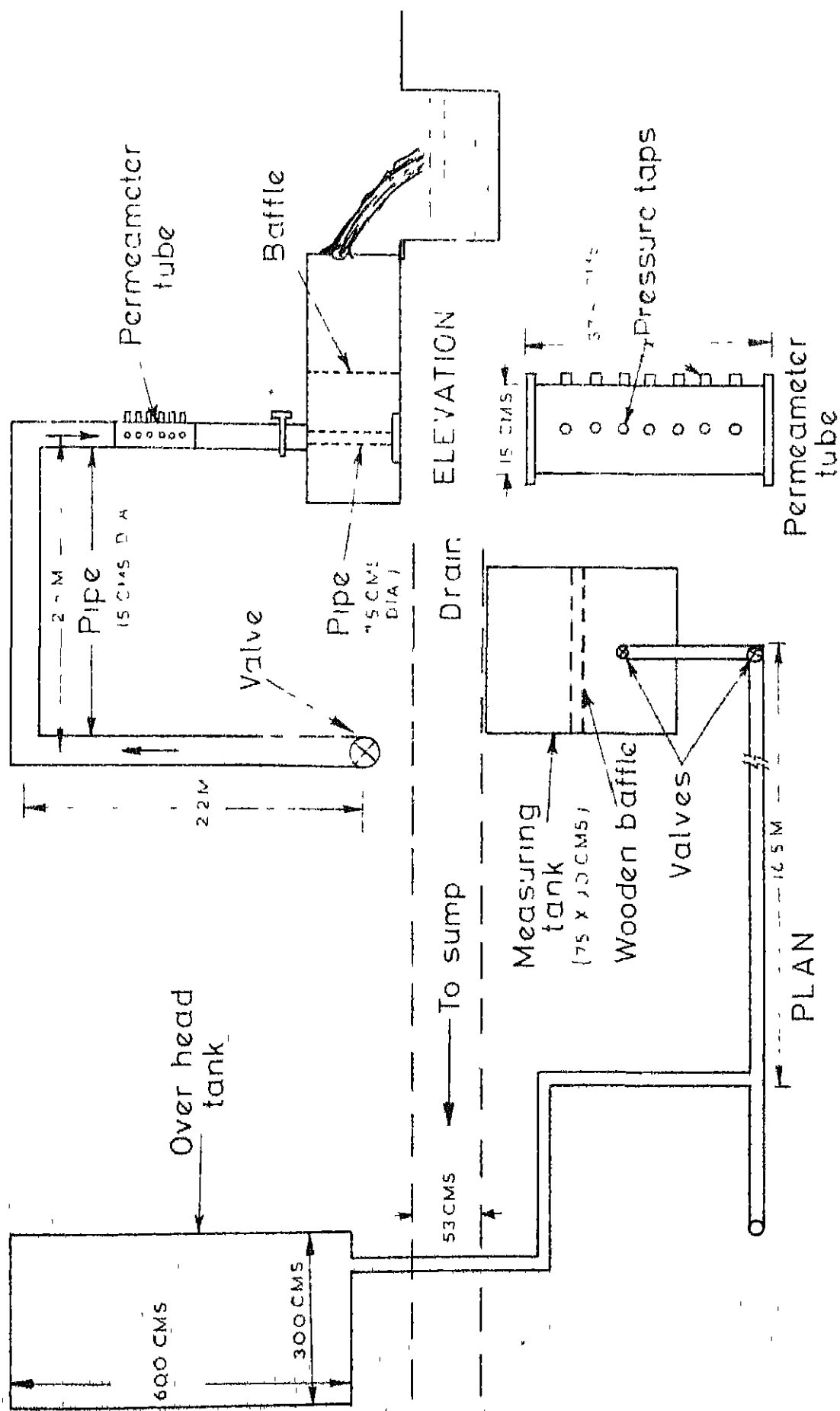


FIG 21

FIG-20 SCHEMATIC DIAGRAM OF THE EXPERIMENTAL SET-UP

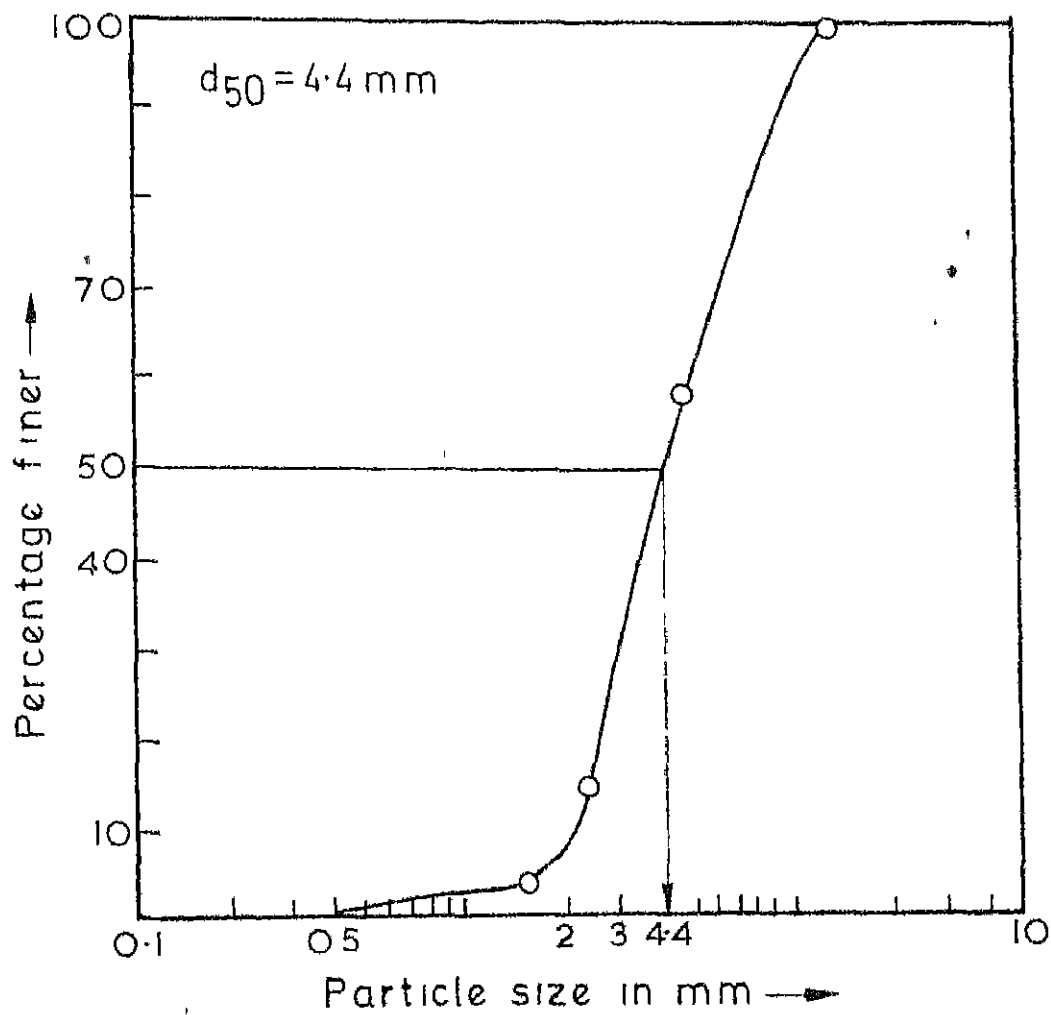


FIG.22 GRAIN SIZE DISTRIBUTION OF RIVER GRAVEL

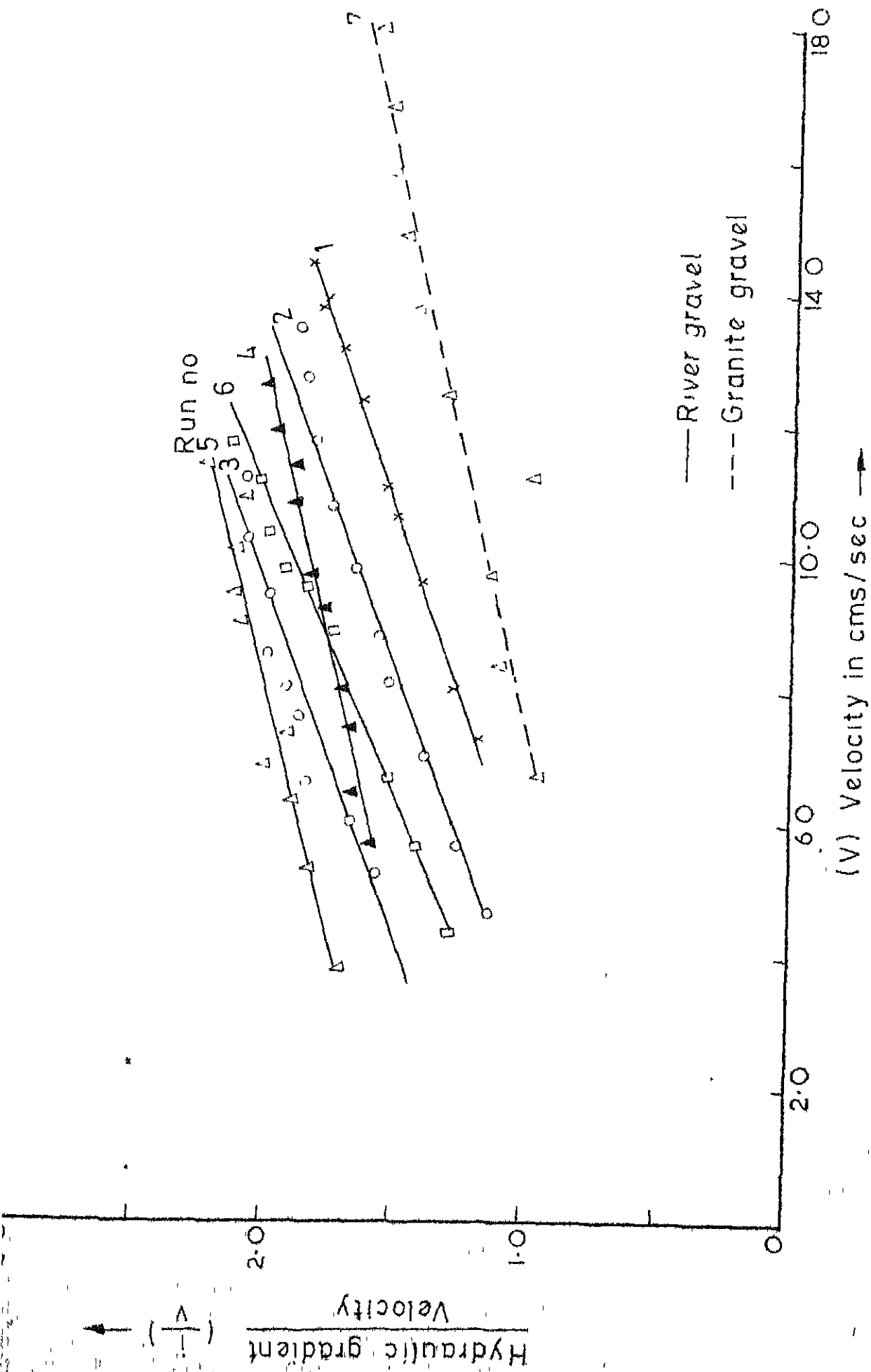


FIG. 23 VARIATION OF $1/V$ WITH V

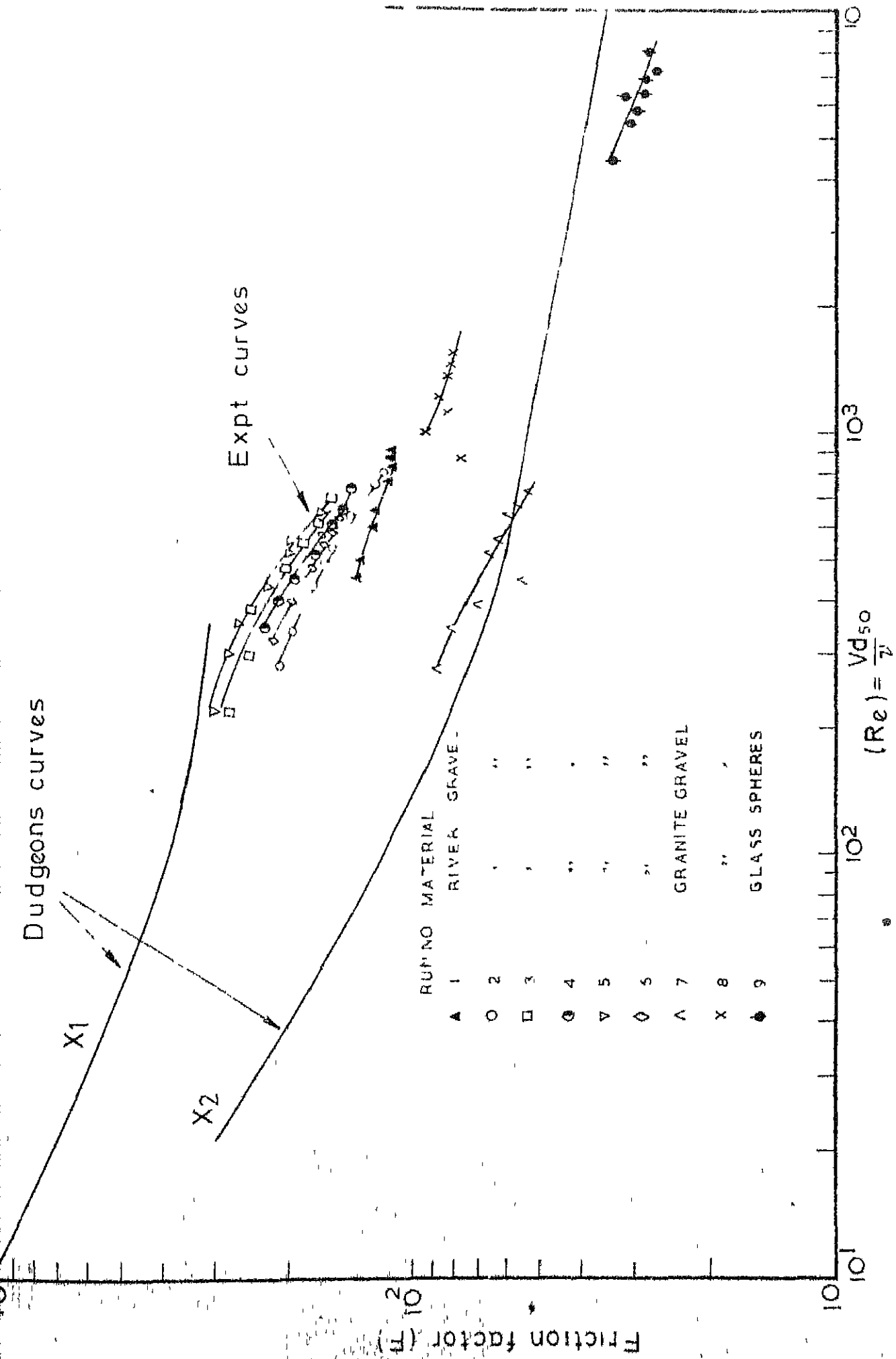


FIG.24 VARIATION OF FRICTION FACTOR WITH REYNOLDS NUMBER

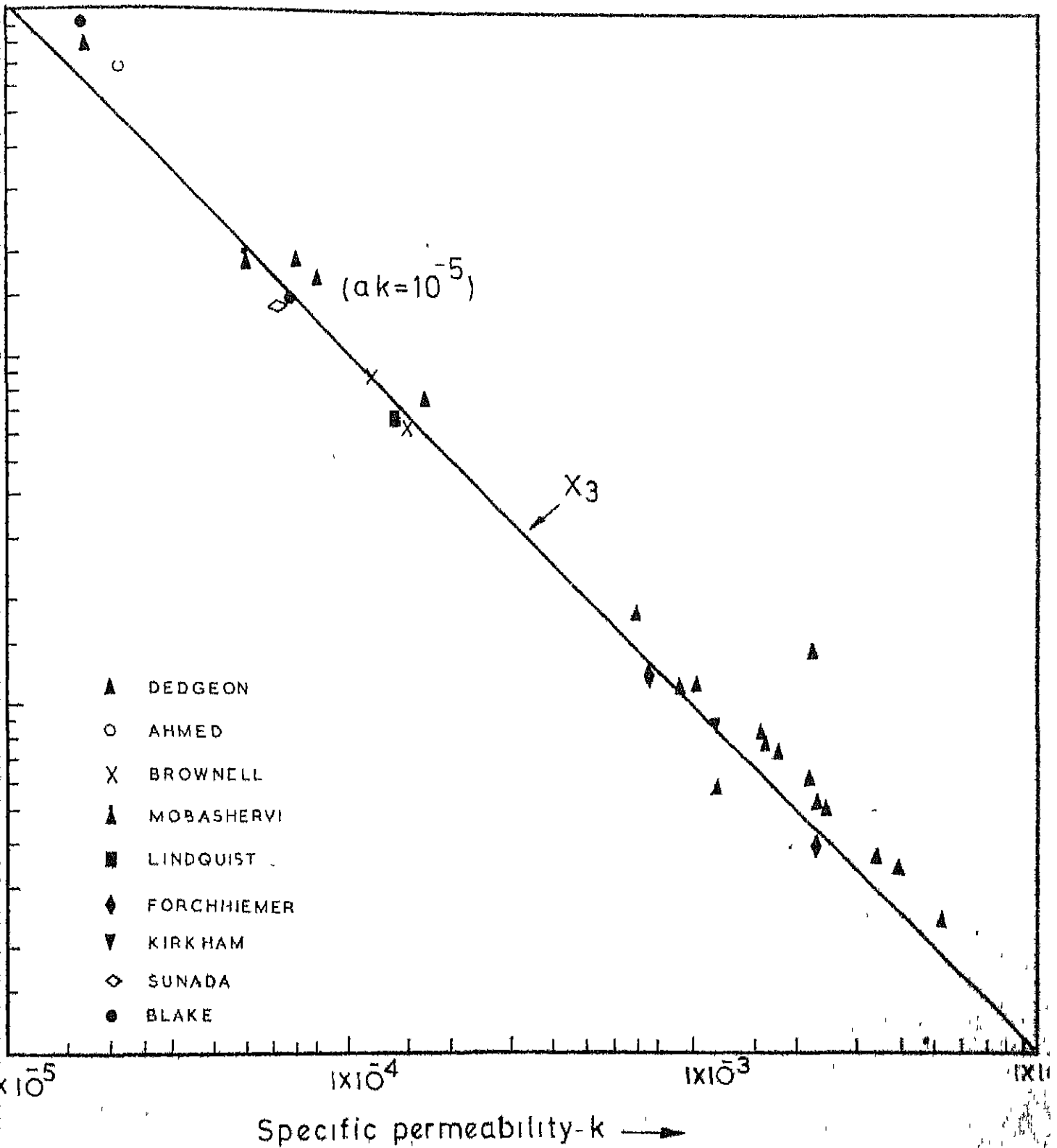


FIG. 25 VARIATION OF COEFFICIENT a WITH SPECIFIC PERMEABILITY k

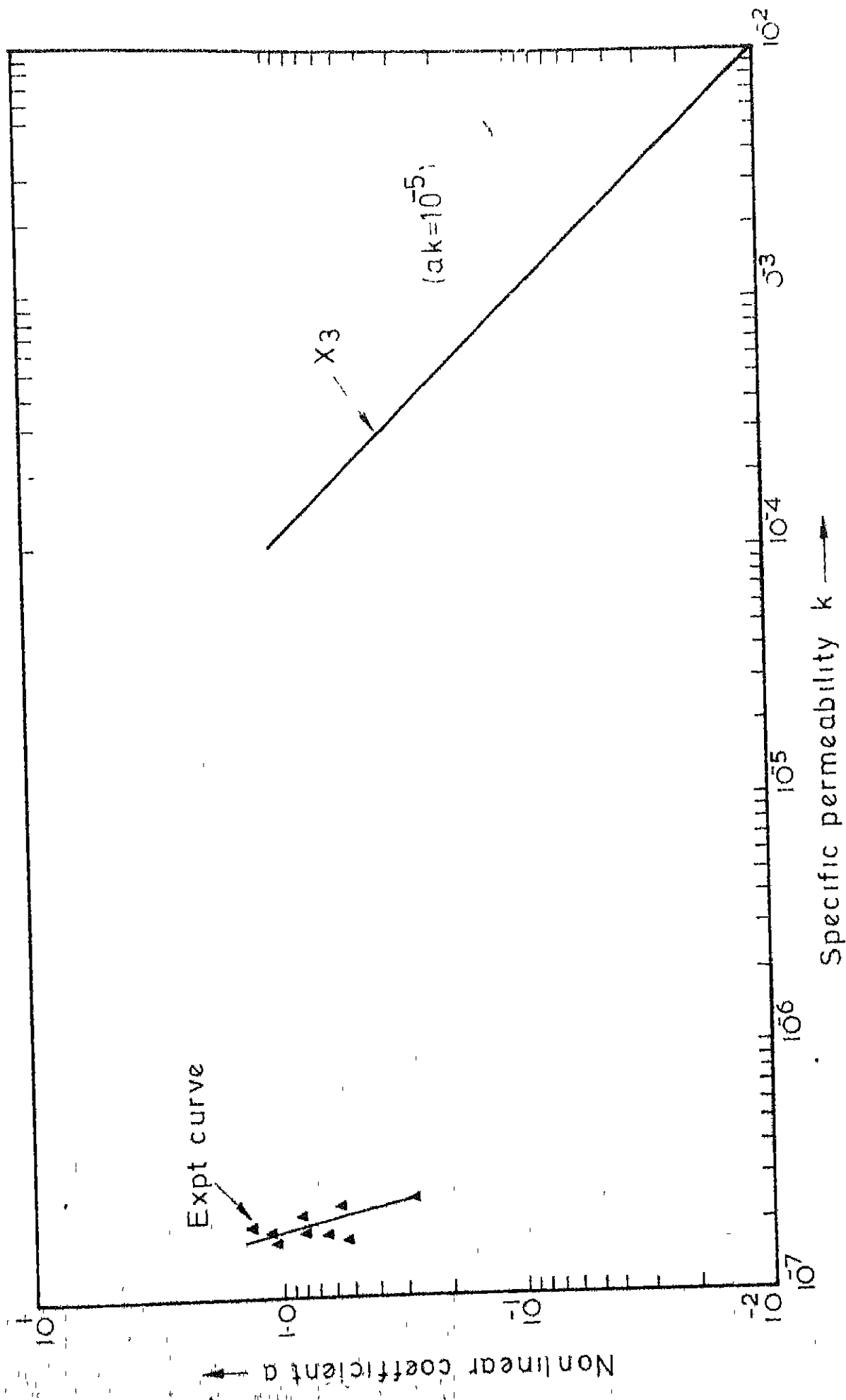


FIG 26 VARIATION OF COEFFICIENT- a WITH SPECIFIC PERMEABILITY- k

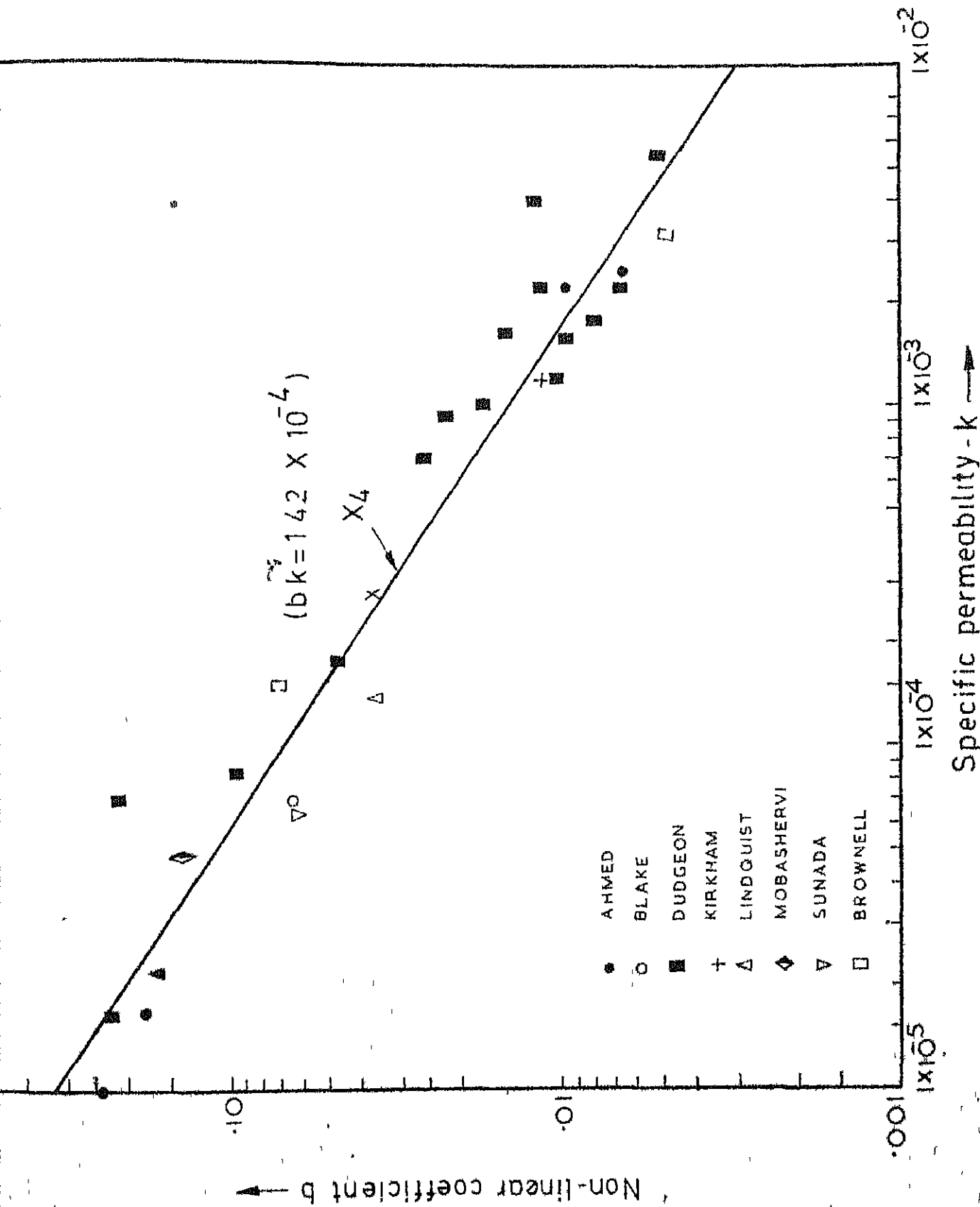


FIG.27 VARIATION OF NON-LINEAR COEFFICIENT b WITH SPECIFIC PERMEABILITY k

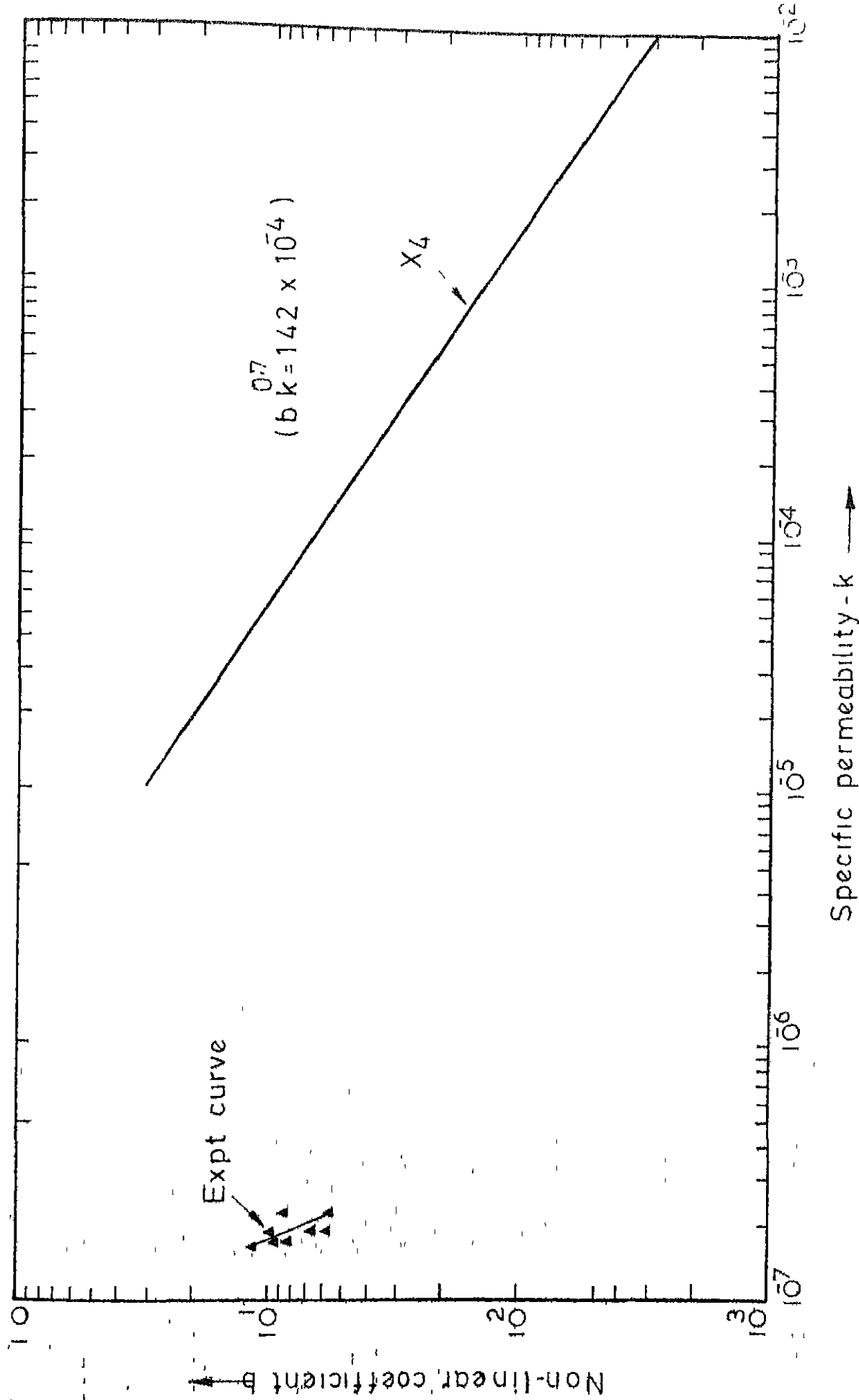


FIG. 28 VARIATION OF NONLINEAR COEFFICIENT b WITH SPECIFIC PERMEABILITY k

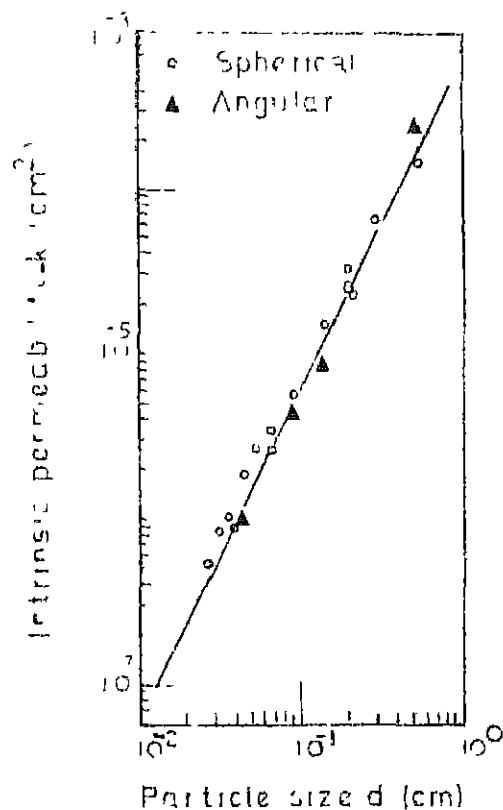


FIG 29 RELATION OF SPECIFIC PERMEABILITY TO PARTICLE SIZE FOR NEARLY UNIFORM POROUS MEDIA (RUMER, R R 1969)

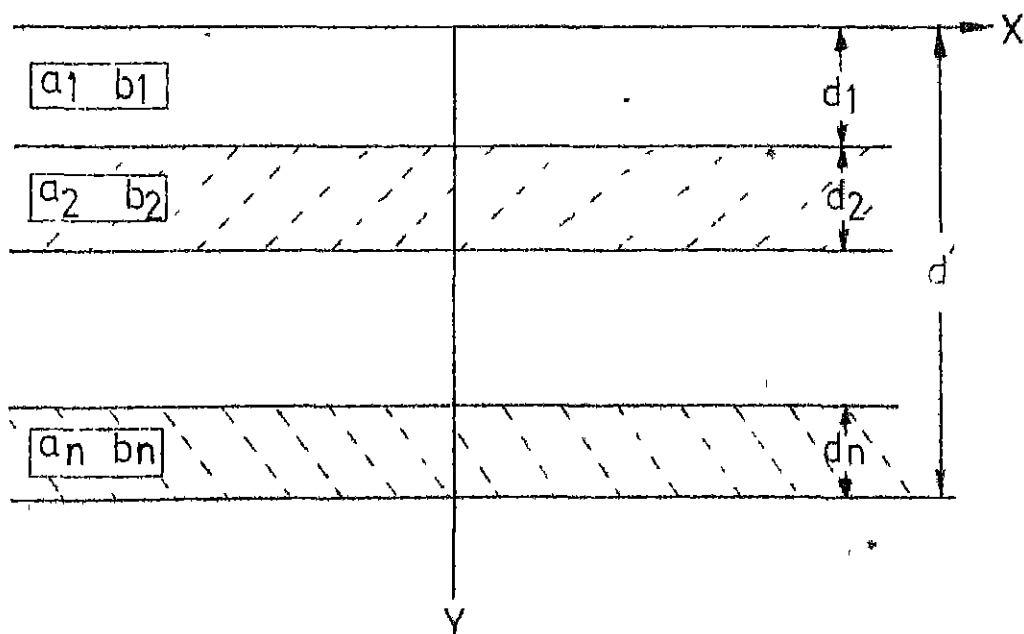


FIG.30 NON HOMOGENEOUS POROUS MEDIA

CHAPTER IV

NON-LINEAR FLOW THROUGH NON-HOMOGENEOUS POROUS MEDIA

4.1 The flow of water through porous media is usually studied assuming that the media is isotropic and homogenous. Often this is not true where gravel and coarse sand of different sizes are used in layers as in filter beds or gravel packs of tube wells. In such cases non-homogeneous medium can be converted into an equivalent single homogenous and isotropic layer for the purpose of analysis. It is advantageous if the equivalent nonlinear permeability coefficients (a, b) of the medium are known. Similar relationships are available for Darcy's law wherein equivalent coefficients of permeability for layered soil can be easily obtained (Hart - 1962).

Figure (30) illustrates a vertical section through a stratified porous media of N their isotropic layers of thickness d_1, d_2, \dots, d_n with nonlinear coefficients $(a_1, b_1), (a_2, b_2) \dots (a_n, b_n)$ respectively.

4.2 Analysis

(a) Flow Parallel to Stratification

For flow in the direction parallel to stratification

the discharge through each layer is governed by the following equations.

$$\begin{aligned}
 i_1 &= a_1 V_1 + b_1 V_1^2 = a_1 \left(\frac{Q_1}{d_1} \right) + b_1 \left(\frac{Q_1}{d_1} \right)^2 \\
 i_2 &= a_2 V_2 + b_2 V_2^2 = a_2 \left(\frac{Q_2}{d_2} \right) + b_2 \left(\frac{Q_2}{d_2} \right)^2 \\
 i_n &= a_n V_n + b_n V_n^2 = a_n \left(\frac{Q_n}{d_n} \right) + b_n \left(\frac{Q_n}{d_n} \right)^2
 \end{aligned} \tag{4.1}$$

Also for horizontal flow

$$i_1 = i_2 = \dots = i_n$$

where i_1, i_2 are hydraulic gradient in successive layers.

For an equivalent single homogenous layer of thickness d' , the hydraulic gradient ' i ' is

$$\begin{aligned}
 i &= i_1 = i_2 = \dots = i_n \\
 &= a_x V + b_x V^2 \\
 &= a_x \left(\frac{Q}{d'} \right) + b_x \left(\frac{Q}{d'} \right)^2
 \end{aligned} \tag{4.2}$$

$$\text{where } d' = d_1 + d_2 + d_3 + \dots + d_n \tag{4.3}$$

Adding N equations given by equation (4.1) leads to

$$\sum_1^N a_n \left(\frac{Q_n}{d_n} \right) + b_n \left(\frac{Q_n}{d_n} \right)^2 = \lambda \left[\sum_1^N a_n \left(\frac{Q_n}{d_n} \right) + b_n \left(\frac{Q_n}{d_n} \right)^2 \right] \quad (4.4)$$

$$\text{Substituting } Q_1 = m_1 Q, Q_2 = m_2 Q, \dots, Q_n = m_n Q. \quad (4.5)$$

$$m_1 + m_2 + \dots + m_n = 1.0$$

$$\sum_1^N m_n = 1.0 \quad (4.6)$$

Substituting for Q_1, Q_2, \dots, Q_n in equation (4.4) and equating the coefficients of equal power of Q to zero.

$$a_x = \frac{1}{N} \left[\sum_1^N \frac{a_n}{d_n} m_n \right] \left(\sum_1^N d_n \right) \quad (4.7)$$

$$\text{and } b_x = \frac{1}{N} \left[\sum_1^N \frac{b_n}{d_n^2} m_n \right] \left(\sum_1^N d_n \right) \quad (4.8)$$

For obtaining the values of m_1, m_2, \dots, m_n , the equation (4.5) is substituted in equation (4.1) to give the following relationships.

$$\frac{a_1}{d_1} m_1 + \frac{b_1}{d_1^2} m_1^2 = \frac{a_2}{d_2} m_2 + \frac{b_2}{d_2^2} m_2^2 = \dots = \frac{a_n}{d_n} m_n + \frac{b_n}{d_n^2} m_n^2 = \lambda \quad (4.9)$$

In equation (4.9), $m_1, m_2 \dots m_n$ are expressed in terms of λ and other known quantities and λ is determined from the relationship

$$\sum_1^N m_n = 1$$

Knowing values of $m_1, m_2 \dots m_n$ the values of a_x and b_x are determined from equations (4.7) and (4.8) respectively.

(b) Flow Normal to Stratification.

In this case, the discharge per unit area of each layer and total head loss through N layers is equal to sum of the head losses in each layer.

$$qd' = \sum_1^N i_n d_n \quad (4.10)$$

$$\text{when } i = a_y V + b_y V^2 \quad (4.11)$$

$$\text{and } i_n = a_n V + b_n V^2 \quad (4.12)$$

Substituting the above relationships of i and i_n and equating the coefficients of equal powers of V to zero, gives following relationships.

$$a_y = \sum_1^N (a_n d_n) / \left(\sum_1^N d_n \right) \quad (4.13)$$

$$\text{and } b_y = \sum_1^N b_n d_n / (\sum_1^N d_n) \quad (4.14)$$

4.3 Experimental Verification - Flow Normal to Stratification

Experiments were conducted on two layers of gravel packed in the permeameter. The size of coarser gravel used was 5.47 m.m. (d_{50}) and finer gravel of size 3.138 m.m. (d_{50}) thickness and the materials were placed at constant height with **densities**, 1.375 gms/cc and 1.305 gms/cc respectively. After saturation, experiments were conducted by varying the head over the permeameter and measuring the gradient and the discharge. The summary of the data are tabulated in the tables (7) and (8a and 8b).

4.4 Results and Discussion :

The head loss obtained for 4 different heads show that there is a good agreement between the head-loss obtained by using the equations 4.10, 4.11 and measured values. The measured head loss and calculated head loss are nearly same, the percentage of error in all the cases are less than 5%, which shows the accuracy with which the above equations can be used to estimate the head loss in layered porous media.

Similarly the same equation can be used to predict the head loss through any number of layered media with known values of coefficient for each layer.

4.5 Head Loss Through Gravel Packs for Tube Wells :

The flow of water through gravel packs for tube wells is governed by non-linear flow equations. It is possible to estimate the head loss through gravel pack (filter pack) for known discharge and pack thickness using Forchheimers equation.

For a tube well drilled in either type of aquifer (uniform or nonuniform) and surrounded by uniform gravel designed on the basis of C.B.I.P. recommendations (Garg - 1970) sand free discharge is assured for gravel pack thickness of about 12.5 cms.

4.6 Analysis for Flow Through Two Layers of Packing :

Let the thickness of packing be t_1 and t_2 . The radius of tube well is r_w , r_1 and r_2 be the radius of the coarser and finer gravel pack respectively.

Let r_{m1} and r_{m2} are the mean radius for inner and outer zone (Fig. 31)

$$r_{m1} = r_1 - t_1/2$$

$$r_{m2} = r_2 - t_2/2$$

$$\text{and } r_m = r_w + (t_1 + t_2)/2$$

where r_m mean radius of the gravel pack

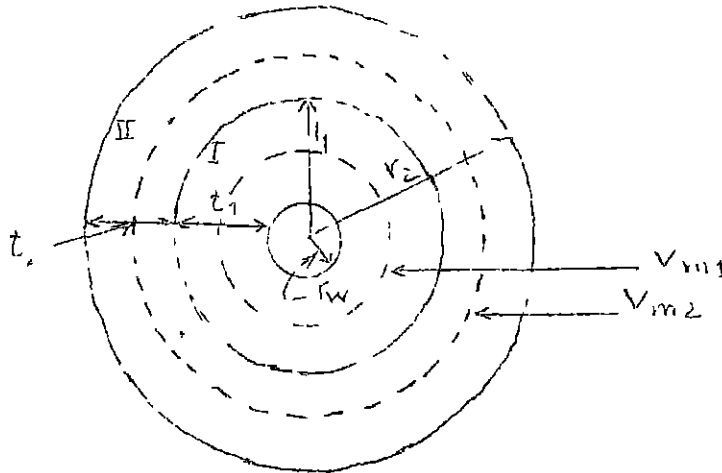


Figure - 31

By continuity discharge through each layer is same

$$Q = 2 \pi r_{m1} V_{m1} = 2 \pi r_{m2} V_{m2} \quad (4.15)$$

where V_{m1} and V_{m2} are the mean velocities at mean radius r_{m1} and r_{m2} respectively.

Head loss through gravel pack layers I and II are given by

$$\begin{aligned} \Delta h_1 &= (a_1 V_{m1} + b_1 V_{m1}^2) t_1 \\ \Delta h_2 &= (a_2 V_{m2} + b_2 V_{m2}^2) t_2 \end{aligned} \quad (4.16)$$

Assuming flow is radial and normal to stratification, equivalent non-linear coefficients for two layers can be found as follows.

Total head loss is

$$= \lambda_1 d_1 + \lambda_2 d_2$$

$$\begin{aligned} (a_y V_m + b_y V_m^2) t' &= (a_1 V_{m1} + b_1 V_{m1}^2) t_1 \\ &+ (a_2 V_{m2} + b_2 V_{m2}^2) t_2 \end{aligned} \quad (4.17)$$

where a_y , b_y are equivalent nonlinear coefficients and V_m mean velocity of flow for entire section. Comparing the coefficients of same power,

$$a_y V_m (t_1 + t_2) = (a_1 V_{m1}) t_1 + (a_2 V_{m2}) t_2$$

$$a_y = \frac{(a_1 V_{m1}) t_1 + (a_2 V_{m2}) t_2}{V_m (t_1 + t_2)} \quad (4.18)$$

$$\text{Similarly } b_y = \frac{(b_1 V_{m1}^2) t_1 + (b_2 V_{m2}^2) t_2}{V_m^2 (t_1 + t_2)} \quad (4.19)$$

$$\text{Since } V_{m1} = \frac{Q}{2 \pi r_{m1}}, \quad V_{m2} = \frac{Q}{2 \pi r_{m2}}, \quad V_m = \frac{Q}{2 \pi r_m}$$

$$a_y = \frac{\left(\frac{a_1 t_1}{r_{m1}} + \frac{a_2 t_2}{r_{m2}} \right)}{(t_1 + t_2)/r_m} \quad (4.20)$$

$$\text{and } b_y = \left(\frac{b_1 t_1}{r_{m1}} + \frac{b_2 t_2}{r_{m2}} \right) / (t_1 + t_2)/r_m \quad (4.21)$$

if $t_1 = t_2$

$$\text{Then } a_y = \frac{\frac{a_1}{r_{m1}} + \frac{a_2}{r_{m2}}}{2/r_m} \quad (4.22)$$

$$b_y = \frac{\frac{b_1}{r_{m1}} + \frac{b_2}{r_{m2}}}{2/r_m} \quad (4.23)$$

Knowing the values of a_y , b_y the equivalent hydraulic gradient (1) and head loss through entire system can be found from the relation

$$hl' = (a_y V_m + b_y V_m^2) (t_1 + t_2) \quad (4.24)$$

CHAPTER V

5.1 Conclusions

In this investigation, many field situations where in non-linear type of flow may occur are highlighted. Solutions to some of the non-linear flow problems are presented using Forchheimer's and Missbach's equations. The solution of these problems indicate that non-linear type of flow, discharge will be less than the discharge under Darcy flow condition. For a given discharge drawdown will be more in case of nonlinear flow.

The experimental investigation shows that there is a good correlation between the nonlinear coefficients a and b and specific permeability k . This correlation can be used to predict the values of a and b for nearly uniform particles with Reynolds number (R_e) range 10-200. The friction factor (F) versus Reynolds number (R_e) can be better represented by different lines for various materials over wide range of Reynolds number (R_e).

The equations are developed for obtaining equivalent nonlinear coefficients for flows both along and normal to the direction of stratification of an N -layered porous media. The experimental verification

shows that there is good correlation between the measured head loss and the head loss obtained from the equations (4.10) and (4.11).

However further analytical and experimental studies are necessary to the solutions of the problems involving higher flow velocities and non homogenous porous media, such as flow through rock fill dams and filter beds.

LIST OF REFERENCES

1. Ahmed, N. and Sunada, D.K., "Non-linear Flow", Journal of Hydraulics Division, ASCE, Proc., Volume 95, November 1969, pp. 1847-1857.
2. Ananda Krishnan, M., and Verda Rajulu, G.H., "Laminar and Turbulent flow of Water Through Sand", Journal of Soil Mechanics & Foundation Engineering, ASCE, Proc. Volume 89, September 1963, pp. 1-15.
3. Dudgeon, C.R., "Well Effects in Permeameters", Journal of the Hydraulic Division. ASCE, Proc. Volume 93, September 1967, pp. 137-148.
4. Garg S.P. "Report of 26th Zonal Meeting of Fundamental and Basic Research", U.P Irrigation Research Institute, Roorkee - February 1970.
5. Horl, M.E., "Ground Water and Seepage", Chapter 1, Fundamentals of Ground Water Flow, McGraw Hill Book Co., INC., Newyork 1962. pp 1-30.
6. Lee, I.K. Lawson, J.D., and Donald, I.B., "Flow of Water in Saturated Soil and Rockfill", Chapter 3 in "Soil Mechanics" - Ed. I.K. Lee, Butterworths, London, 1968. pp. 82-110.

7. Leonards, C.A., "Foundation Engineering", Chapter 3, De-watering, McGraw Hill Book Co., INC., New York 1962, pp 241-350.
8. Madhav H.R. and Subramanya K. - "Nonlinear Flow Through Porous Media", Proc 40th Annual Research Session, CBIP (India), Volume 1-C, June 1970.
9. Parkin, A.K., "Rockfill Dams with Inbuilt Spillways - Hydraulic Characteristics" - Water Research Foundation of Australia Bulletin No.6, February 1963.
10. Parkin, A.K., Trollope, D.H., & Lawson, J.D., "Rockfill Structures Subject to Water Flow" Journal of Soil Mechanics & Foundation Engineering. Proc ASCE Volume 92, S.M. 6, November 1966.
11. Parkin A.K. and Ian C.O' Neill - "Discussion of Nonlinear Flow in Porous Media - Journal of Hydraulic Division, Proc. ASCE, July 1970, pp. 1632-33.
12. Ranganadha Rao, B.P., Suresh C., Todd D.K., & Tyagi, A.K., "Discussion of Nonlinear Flow Through Porous Media", Journal of Hydraulic Division. Proc. ASCE., August 1970, pp. 1732-1738.
13. Rubie J.B. " An electrical analogue for some cases of Nonlinear Flow through Porous Media". Journal of Hydraulic Research, Volume 4, 1966, No.2, pp. 1-20.

14. Rubiac J.B., "The Study of Nonlinear Flow Through Porous Media by Means of Electrical Models" Journal of Hydraulic Research, Volume 7, 1969, No.1, pp. 31-65.
15. Rumer R.R. Jr. "Flow Through Porous Media", Chapter-3 Resistance to Flow in Porous Media. Edited by De Wiest R.J.Jr. Academic Press Newyork 1969. pp. 99-100.
16. Robin, P.C., and Larson J.D., "Flow Over and Through Rockfill Banks". Journal of Hydraulic Division. Proc. ASCE. Volume 93, September 1967, pp. 1-21.
17. Taylor, D. L., "Fundamentals of Soil Mechanics". John Wiley & Sons, Inc. Newyork, - 1957.
18. Todd D.P., "Ground Water Hydrology" - John Wiley & Sons, Inc. Newyork - 1959.
19. Volker R.E., "Nonlinear Flow in Porous Media by Finite Elements". Journal of Hydraulic Division. Proc. ASCE, Volume 95, November 1969, pp. 2093-2114.
20. Wilkins J.K., "The Flow of Water Through Rockfill and its Application to the Design of Dams". Newzealand Engineering. 10:11, 1955.
21. Wright, D.E., "Nonlinear Flow in Porous Media". Journal of Hydraulic Division, Proc. ASCE., Volume 94, July 1968, pp 851-872.

APPENDIX - A

TABLE 1

(DATA OF DUDGEON-1964)

Sl. No.	a sec./cms	b sec. ² /cm ²	Medium	Stand ard error in S_y	Specific Permeab- ility k cm. ²	Particle size in cms.
1	2	3	4	5	6	7
1	0.0115	0.0162	Blue Metal	.0020	1.03×10^{-3}	1.1
2	0.0073	0.0077	Marble Mixture	.0006	1.75×10^{-3}	1.58
3	8.1161	-0.0961	Nepean Sand	2.0478	1.66×10^{-6}	0.027
4	0.1904	0.2174	River Gravel	.0029	7.07×10^{-5}	0.2
5	0.7891	0.2232	River Gravel	.2873	1.69×10^{-5}	0.095
6	0.1661	0.095	Blue Metal	.1184	8.05×10^{-5}	0.19
7	0.0779	0.0573	Blue Metal	.034	1.72×10^{-4}	0.47
8	0.0024	0.0051	River Gravel	.0005	5.4×10^{-3}	4.0
9	0.0033	0.0121	Blue Metal	.0008	4.0×10^{-3}	2.50
10	0.0082	0.0145	River Gravel	.0032	1.62×10^{-3}	1.2
11	0.0189	0.0262	Blue Metal	.0067	7.0×10^{-4}	1.9
12	0.0061	0.0117	Blue Metal	.0018	2.2×10^{-3}	1.82

1	2	3	4	5	6	7
12	0.0061	0.0117	Blue Metal	.0018	2.2×10^{-3}	1.8
13	0.0143	0.22	Blue Metal	.0034	9.2×10^{-4}	1.05
14	0.011	0.0103	Marbles	.0017	1.2×10^{-3}	1.56
15	0.0058	0.0066	Marbles	.0042	2.24×10^{-3}	2.46
16	0.00064	0.0015	River Gravel	.0003	2.47×10^{-3}	8.4
17	0.005	0.0063	Marbles	.0001	1.56×10^{-3}	1.56
18	0.0076	0.0095	Marbles	.00018	1.73×10^{-3}	1.56
19	0.0051	0.0097	Blue Metal	.0007	2.3×10^{-3}	1.05
20	0.0036	0.0049	Marbles	.0014	3.18×10^{-3}	2.85

TABLE 2

(DATA OF AHMED & GUNADA-1969)

Sl. No.	Investigator	a sec./cms	b sec. ² /cm ²	Medium	Stand ard error S _y	Specific Permeab- ility k cm. ²	Particle size in cms.
1	2	3	4	5	6	7	8
1	Ahmed	7.39	0.745	Sand	1.5	2.1x10 ⁻⁶	0.054
2	Ahmed	3.8	0.454	Sand	1.7	3.96x10 ⁻⁶	0.0764
3	Ahmed	2.3	0.308	Sand	1.0	6.91x10 ⁻⁶	0.107
4	Ahmed	1.49	0.24	Sand	2.5	1.0x10 ⁻⁵	0.14
5	Ahmed	0.938	0.179	Sand	1.0	1.69x10 ⁻⁵	0.199
6	Ahmed	0.694	0.165	Sand	2.0	2.21x10 ⁻⁵	0.258
7	Allen	1.47	0.142	Granular Absorbent	3.3	8.6x10 ⁻⁶	0.0855
8	Blake	0.149	0.0623	Glass Beads	1.6	6.7x10 ⁻⁵	0.32
9	Brownell	0.0647	0.0183	Glass Beads	1.4	1.5x10 ⁻⁴	0.53
10	Brownell	0.089	0.021	Nickel Saddles	5.0	1.12x10 ⁻⁴	0.334

1	2	3	4	5	6	7	8
11	Francher	16.6	7.96	Ottawa Sand	4.1	8.2×10^{-7}	0.07
12	Forchhammer	0.00408	0.0005	Sand	2.2	2.3×10^{-3}	0.5
13	Forchhammer	0.0123	0.00092	Sand	2.1	7.6×10^{-4}	0.3
14	Kirkham	0.00895	0.0117	Marble	4.1	1.19×10^{-3}	1.6
15	Lindquist	0.0674	0.0368	Sand	3.0	1.38×10^{-4}	0.492
16	Lindquist	1.164	0.292	Sand	4.5	8.0×10^{-6}	0.105
17	Mohasheri	0.189	0.137	Sand	6.5	4.94×10^{-5}	0.5
18	Sun do	0.145	0.064	Glass Spheres	4.4	6.45×10^{-5}	0.3

TABLE 3

(DATA OF RANGANADHA RAO AND SURESH-1970)

Sl. No.	a sec./cms	b Sec. ² /cm ²	Medium	Porosity (n)	Specific Permeability k cm. ²	Particle size in cms.
1	2	3	4	5	6	7
1	0.099	0.263	River Gravel Fairly Round	.40	7.30×10^{-6}	0.101
2	1.15	0.345	"	.381	6.53×10^{-6}	0.101
3	0.325	0.11	"	.436	22.54×10^{-6}	0.17
4	0.475	0.199	"	.417	15.90×10^{-6}	0.17
5	0.400	0.164	"	.403	18.78×10^{-6}	0.17
6	0.515	0.333	"	.392	14.88×10^{-6}	0.17
7	0.135	0.072	"	.430	56.65×10^{-6}	0.286
8	0.225	0.088	"	.423	34.60×10^{-6}	0.286
9	0.540	0.400	"	.403	22.10×10^{-6}	0.286

1	2	3	4	5	6	7
10	0.075	0.053	River Gravel Fairly Round	.384	9.79×10^{-6}	0.404
11	0.105	0.078	"	.367	68.47×10^{-6}	0.404
12	0.043	0.043	"	.372	165.8×10^{-6}	0.55
13	0.074	0.055	"	.456	102.80×10^{-6}	0.55
14	0.105	0.078	"	.346	73.38×10^{-6}	0.55

TABLE 4

(DATA OF ANANDAKRISHNAN & VARDARAJU-1963)

Sl. No.	Medium	m	$1/C = (K')$ C.G.S. Units
1	2	3	4
1	Coarse Sand	1.11	4.14×10^{-2}
2	"	1.3	2.43×10^{-2}
3	"	1.63	2.44×10^{-2}
4	Medium Sand	1.07	3.12×10^{-2}
5	"	1.26	1.89×10^{-2}
6	"	1.48	1.75×10^{-2}
7	Fine Sand	1.11	0.55×10^{-2}
8	"	1.60	0.069×10^{-2}
9	Very Fine Sand	1.00	0.170×10^{-2}
10	"	1.07	0.147×10^{-2}

TABLE 5

PHYSICAL PROPERTIES OF POROUS MEDIA

Run No.	Medium	a secs./cms	b secs. ² /cms ²	Porosity	Specific Permeability k cm. ²	Particle size (d ₅₀) cms	Reynolds number Range Re
1	2	3	4	5	6	7	8
1	River Gravel	0.5076	0.0855	.40	1.72×10^{-7}	0.44	452-890
2	"	0.675	0.10	.39	1.785×10^{-7}	0.44	275-807
3	"	1.096	0.0961	.363	1.67×10^{-7}	0.44	212-627
4	"	1.267	0.058	.386	1.83×10^{-7}	0.44	333-770
5	"	1.465	0.067	.394	1.905×10^{-7}	0.44	212-633
6	"	0.800	0.1125	.366	1.72×10^{-7}	0.44	317-663
7	Granite Gravel	0.57	0.06	.465	2.24×10^{-7}	0.318	272-732
8	"	0.283	0.0916	.45	2.3×10^{-7}	0.57	657-1549
9	Glass Spheres	0.105	0.007	.396	-	1.5	4500-7577

TABLE 6

SUMMARY OF THE EXPERIMENTAL RESULTS

Sl. No.	Run No.	Q Lit./Sec.	V Cms./Sec.	α	R_e (Vd_{50}) $= \frac{R_e}{\Delta}$	F $= \frac{2gd_{50}^3}{V^2}$
1	2	3	4	5	6	7
1	1	1.989	10.54	15.70	653.75	122.0
2	"	2.31	12.24	20.10	759.2	115.8
3	"	2.462	13.05	22.40	809.44	113.55
4	"	2.58	13.67	25.20	847.9	116.42
5	"	2.709	14.35	27.00	990.07	113.2
6	"	1.505	7.97	10.2	494.35	138.62
7	"	1.81	9.59	13.50	594.83	126.72
8	"	2.072	10.97	17.20	620.42	123.38
9	"	1.376	7.29	8.48	452.17	137.75
10	"	2.604	13.80	23.80	855.96	107.89

1	2	3	4	5	6	7
11	2	2.556	13.54	25.20	807.16	118.66
12	"	2.386	12.64	23.00	753.50	124.27
13	"	2.20	11.66	21.40	695.09	135.88
14	"	2.003	10.61	18.60	632.49	142.63
15	"	1.849	9.80	16.50	584.20	148.30
16	"	1.66	8.79	13.80	524.00	154.18
17	"	1.534	8.31	12.50	484.70	163.22
18	"	1.322	7.00	9.80	417.30	172.65
19	"	1.067	5.65	7.24	336.81	195.79
20	"	0.872	4.62	5.16	275.41	201.70

1	2	3	4	5	6	7
21	3	2.10	11.12	23.80	627.90	166.16
22	"	1.915	10.148	21.50	573.02	180.23
23	"	1.778	9.42	19.20	531.91	186.79
24	"	1.593	8.44	17.30	476.57	209.66
25	"	1.517	8.03	15.50	453.42	206.17
26	"	1.239	6.56	12.30	370.42	246.74
27	"	1.426	10.55	13.90	426.32	210.51
28	"	1.139	6.03	9.97	340.49	236.71
29	"	0.712	3.77	4.67	212.87	283.65
30	"	0.980	5.19	8.10	293.06	259.59

1	2	3	4	5	6	7
31	4	2.03	10.76	20.30	625.49	151.36
32	4	1.843	9.76	17.90	567.36	162.22
33	"	1.722	9.12	16.00	530.16	166.06
34	"	1.523	8.07	13.75	469.12	182.26
35	"	1.393	7.38	12.70	429.00	201.30
36	"	1.081	5.73	9.20	330.10	241.89
37	"	1.213	6.43	10.80	373.78	225.50
38	"	2.128	11.28	21.10	655.72	143.15
39	"	2.229	11.81	23.20	686.53	143.59
40	"	2.370	12.56	26.30	730.13	143.92

1	2	3	4	5	6	7
---	---	---	---	---	---	---

41	5	1.355	7.18	13.00	400.48	217.69
42	"	2.143	11.35	25.20	633.07	168.87
43	"	2.051	10.87	22.80	606.30	166.58
44	"	1.395	10.04	21.40	560.00	183.27
45	"	1.778	9.42	20.60	525.42	200.41
46	"	1.183	6.27	11.90	349.72	261.31
47	"	0.998	5.29	9.30	295.06	286.89
48	"	0.719	3.81	5.07	212.51	301.51
49	"	1.691	8.96	18.90	499.76	203.23
50	"	1.376	7.29	13.80	406.61	224.17

1	2	3	4	5	6	7
51	6	1.053	5.579	7.95	317.78	220.49
52	"	1.529	8.10	13.60	461.32	178.94
53	"	1.66	8.79	15.45	506.79	172.62
54	"	1.778	9.42	17.40	536.56	169.27
55	"	2.093	11.09	22.40	631.68	157.23
56	"	2.20	11.657	25.40	663.98	161.36
57	"	1.942	10.29	20.70	586.11	168.76
58	"	1.817	9.627	19.10	548.35	177.91
59	"	1.239	6.56	10.00	373.65	200.60
60	"	1.076	5.70	5.70	324.67	151.45

1	2	3	4	5	6	7
---	---	---	---	---	---	---

61	7	2.10	11.13	10.90	453.00	54.20
62	"	3.395	17.99	28.20	732.21	53.68
63	"	3.166	16.79	26.30	683.36	57.47
64	"	2.962	15.69	24.10	638.59	60.31
65	"	2.784	14.75	21.40	600.33	60.59
66	"	2.588	13.71	19.45	558.00	63.74
67	"	2.348	12.43	16.50	505.91	60.79
68	"	1.836	9.73	11.05	396.02	71.90
69	"	1.599	8.475	9.45	344.90	81.05
70	"	1.264	6.70	6.44	272.69	88.38

1	2	3	4	5	6	7
---	---	---	---	---	---	---

71	8	2.928	15.51	18.40	1038.0	82.08
72	"	2.229	11.81	10.25	866.57	78.86
73	"	1.691	8.96	4.81	657.45	64.30
74	"	2.517	13.34	15.70	978.84	94.68
75	"	3.442	18.24	26.00	1338.0	83.87
76	"	3.148	16.68	23.30	1223.0	89.87
77	"	3.704	19.62	29.80	1439.0	83.08
78	"	3.987	21.12	34.20	1549.0	82.28
79	"	3.834	20.31	31.50	1490.0	81.95
80	"	3.509	18.59	26.30	1364.0	81.67

1	2	3	4	5	6	7
<hr/>						
81	9	7.111	37.67	13.50	7216	28.00
82	"	7.467	39.56	14.60	7578	27.45
83	"	8.006	42.41	17.30	8123	28.30
84	"	7.741	41.01	15.15	7855	26.51
85	"	6.85	36.29	12.80	6951	28.60
86	"	6.47	34.28	11.90	6566	29.80
87	"	5.971	31.63	11.05	6058	32.50
88	"	5.724	30.32	9.45	5808	30.25
89	"	5.371	28.45	8.62	5450	31.34
90	"	4.436	23.50	6.44	4501	34.32

TABLE 7

PHYSICAL PROPERTIES OF THE CHAIRMAN GRAVEL

Material	Layer I	Porosity(n)	Layer II	Porosity
Granite	Size	.	Size	
Gravel	4.7-6 25 mm	.48	1.656-4.7 mm	.505

TABLE 8 (a)

SUMMARY OF THE EXPERIMENTAL RESULTS

Run No.	Q c.c.	V cms	R _e	1_1	a_1 sec. ² / cms.	b_1 sec. ² / cms.
10	3509	18.59	756	28.8	1.286	0.0143
10	3443	18.24	742	28.2	1.286	0.0143
10	3023	16.02	651	24.3	1.299	0.0138
10	3229	17.11	696	26.3	1.299	0.0138

TABLE 8 (b)

SUMMARY OF DATA FOR THE TOTAL FLOW

R_e	l_2	a_2 sec./ cms	b_2 sec. ² / cms ²	a_y sec./ cms.	b_y sec. ² / cms. ²	Calcu lated Head Loss in cms.	Meas ured Head Loss in cms.	Perce ntage error
1564	21.1	0.869	0.0143	1.025	0.0145	425	432	1.75
1338	20.6	0.869	0.0143	1.025	0.0143	415	399	3.86
1178	17.25	0.765	0.0201	0.965	0.0178	354	339	4.25
1254	19.00	0.765	0.0201	0.965	0.0178	382	389	1.95

APPENDIX B

HEAD LOSS THROUGH GRAVEL PACK OF A TUBE WELL

In this appendix, the calculation of head loss through gravel pack of a tube well using the equation (4.24) is illustrated with a simple example.

For a tube well of diameter 15 cms. with gravel pack thickness of 12.5 cms and aquifer particle size of 0.5 m.m. (medium sand), the discharge is 20 litres per metre length of the screen Fig. (32).

In this case, equation (4.24) simplifies to

$$id' = aV_m + bV_m^2$$

where V_m is the mean velocity at radial distance r_m from the centre of the well.

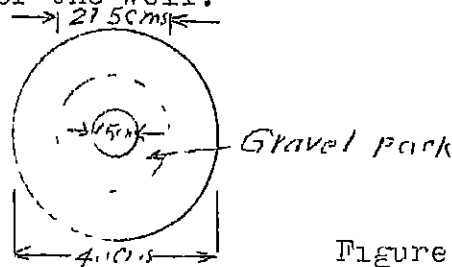


Figure - 32

r_m = Mean radius of the gravel pack.

Discharge = Average area of flow x mean velocity.

$$20 \times 10^3 = 2 \pi \times 27.5 \times 100 V_m$$

$$V_m = 2.31 \text{ cm/sec.}$$

Assuming pack aquifer ratio as 12.0 (Garg - 1970).

Gravel pack size = $12 \times 0.5 = 6 \text{ m.m.}$

Value of coefficients a and b for gravel pack of 6 m.m. size are assumed as .065 and .042 respectively.

Substituting the values of a, b and V_m in equation,

Head loss = 4.52 cms.

APPENDIX C

WALL EFFECT IN PERMEAMETER

The laboratory methods of the permeabilities measurements of porous materials is carried out in permeameter of finite cross section. The sample is bounded by a smooth wall which is impermeable. The presence of smooth wall affects the flow behaviour adjacent to the wall which in turn affects the velocity for a thin zone near the wall is higher than that for inner zone mainly due to the higher porosity near the wall zone.

In the present analysis the flow is assumed to follow linear law in the inner zone and for wall zone where velocity is higher the flow is governed by non-linear law. Dudgeon (1967) estimated the wall effect in permeameter with some assumptions and using the power law equation (1.3).

Figure (33) shows cross section of a permeameter.

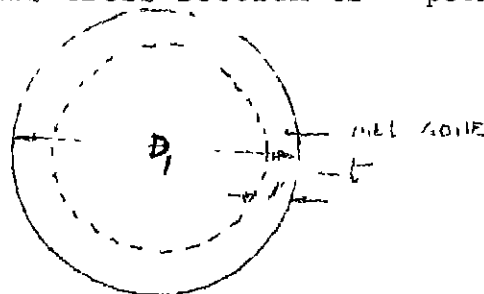


Figure 33

Let D_1 be the diameter of permeameter and t , width of
 an wall zone

A_1 = Cross sectional area of inner zone ($D_1 - 2t$) in
 diameter

A = Total Area

$A_w = A - A_1$
 = Wall Zone Area

For Inner Zone

$$i = \frac{V_1}{K} \dots\dots (C1)$$

V_1 = Velocity in the inner zone

For wall zone, using equation (1.2)

$$i = a_w v_w + b_w v_w^2 \dots\dots (C2)$$

where a_w, b_w are nonlinear coefficients for wall zone and
 v_w velocity through wall zone. Since hydraulic gradient
 to inner and outer zones are same.

$$\frac{V_1}{K} = a_w v_w + b_w v_w^2 \dots\dots (C.4)$$

$$b_w v_w^2 + a_w v_w - \frac{V_1}{K} = 0 \dots\dots (C.5)$$

Solving the quadratic equation (C.5) for V_w and taking positive sign,

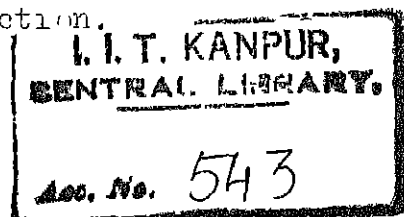
$$V_w = \frac{-a_w + \sqrt{a_w^2 + \frac{4b_w \bar{V}_1}{K}}}{2b_w} \quad (C.6)$$

$$V_m = \frac{4 \frac{V_w}{V_1} (D_1 t - t^2) + (D_1 - 2t)^2}{D_1^2} \quad (C.7)$$

Substituting equation (C.6) in (C-7)

$$\frac{V_m}{V_1} = \left(\frac{8 (D_1 t - t^2)}{K a_w (1 + \sqrt{1 + \frac{4 \bar{V}_1 b_w}{K a_w^2}})} + (D_1 - 2t)^2 \right) / D_1^2 \quad (C.8)$$

V_m = Mean velocity for entire section.



CE-1971-M-RAO-NON

Thesis
532.51
R18

543

Rao,
Nonlinear flow through
porous media.

Date

子

4

[illegible]